Fakultät für Medizin

Abteilung für Nuklearmedizin

Abteilung für diagnostische und interventionelle Neuroradiologie

Multimodal neuroimaging on neurodegenerative disorders using the hybrid PET/MRI technique

Masoud Tahmasian

Vollständiger Abdruck der von der Fakultät für Medizin der Technischen Universität München zur Erlangung des akademischen Grades eines

Doctor of Philosophy (Ph.D.)

genehmigten Dissertation.

Vorsitzender: Univ.-Prof. Dr. Arthur Konnerth

Betreuer: Univ.-Prof. Dr. Alexander Drzezga

Prüfer der Dissertation:

1. Univ.-Prof. Dr. Claus Zimmer

2. Priv.-Doz. Dr. Markus Ploner

Die Dissertation wurde am 03.06.2014 bei der Fakultät für Medizin der Technischen Universität München eingereicht und durch die Fakultät für Medizin am 18.08.2014 angenommen.

To

My Family

INDEX

INDEX

LIST OF ABBREVIATIONS

Aβ	Amyloid beta
AD	Alzheimer's disease
APOE	Apolipoprotein E
APP	Amyloid precursor protein
BOLD	Blood-oxygen-level-dependent
bvFTD	Behavioral variant frontotemporal dementia
CDR	Clinical dementia rating
CON	Healthy controls
CSF	Cerebrospinal fluid
DC	Degree centrality
DMN	Default mode network
DSM	Diagnostic and Statistical Manual of Mental Disorders
DTI	Diffusion tensor imaging
EPI	Echo planar imaging
FC	Functional connectivity
FDG	Fluorodeoxyglucose
Fig.	Figure
fMRI	Functional magnetic resonance imaging
FoV	Field of view
FTLD	Frontotemporal lobar degeneration
GMV	Gray matter volume
HP	Hippocampus
iFC	Intrinsic functional connectivity
IFG	Inferior frontal gyrus

LT	Left temporal lobe
MCI	Mild cognitive impairment
MDD	Major depressive disorder
MMSE	Mini mental state examination
MPRAGE	Magnetization prepared rapid gradient echo
MRI	Magnetic resonance imaging
MTL	Medial temporal lobe
NDH	Network degeneration hypothesis
NINCDS-ADRDA	National Institute of Neurological and Communicative Disorders and Stroke and the Alzheimer's Disease and Related Disorders Association
NFT	Neurofibrillary tangle
PCC	Posterior cingulate cortex
PET	Positron emission tomography
PiB	Pittsburgh compound B
PNFA	Progressive nonfluent aphasia
RAng	Right angular
RFI	Right frontoinsula
ROI	Region of interest
RSC	Retrosplenial cortex
rs-fMRI	Resting state fMRI
SD	Sementic dementia
sMRI	Structural MRI
SNR	Signal to noise ratio
Tab.	Table
VBM	Voxel based morphometry

Abstract:

Simultaneous evaluation of intrinsic functional connectivity and local metabolic activity using a hybrid positron emission tomography/magnetic resonance imaging (PET/MRI) offers a new in-vivo tool to provide both better understanding of the pathogenesis and diagnostics of neurodegenerative disorders. In the current thesis, first steps into this direction have been realized with respect to Alzheimer's disease and frontotemporal lobar degeneration. Particularly, I have studied changes in multimodal properties of different brain regions in two different projects on these disorders:

In project one, the relationship between local glucose metabolism, functional connectivity, and grey matter volume of the hippocampus and precuneus has been studied in 40 patients with Alzheimer's disease-dementia, 21 patients with mild cognitive impairment and 26 healthy subjects. I used 18F-fluorodesoxyglucose-PET to measure local glucose metabolism, resting-state functional MRI and seed-based functional connectivity analysis to measure intrinsic functional connectivity, and structural MRI and voxel-based morphometry to estimate regional brain volumes. Group comparisons were corrected for the effects of atrophy, age, gender and also partial volume effect. The findings demonstrated that in patients, intrinsic connectivity between hippocampus and precuneus was reduced. Patients' metabolism was progressively reduced in the precuneus, while it was unchanged in the hippocampus. Critically, for patients with Alzheimer's disease-dementia hippocampal metabolism was negatively correlated with connectivity between hippocampus and precuneus. Results provided the first evidence for an inverse relationship between intra-hippocampal metabolism and extra-hippocampal intrinsic connectivity in Alzheimer's disease. Data are consistent with the hippocampus disconnection hypothesis of Alzheimer's disease.

The second project: it has been demonstrated that each neurodegenerative disorder affects preferentially specific brain networks and my hypothesis was that the network degeneration hypothesis of neurodegenerative diseases can help to separate individual patients with Alzheimer's disease and 3 main subtypes frontotemporal lobar degeneration, namely, semantic dementia, progressive non-fluent aphasia, and behavioral variant frontotemporal dementia. Forty

patients with simultaneous resting-state functional MRI, structural MRI, and 18F-fluorodesoxyglucose were assessed in the hybrid PET/MRI scanner. Afterwards, I measured voxel-wise degree centrality values as a surrogate for intrinsic functional connectivity, voxel-wise regional glucose metabolism values as a surrogate for effective neuronal activity and voxel-wise voxel-based morphometry values as a surrogate for regional gray matter volume within the main cores of four intrinsic networks that are primarily affected by those four diseases based on the network degeneration hypothesis. Subsequently, support vector machine was applied to classify each patient from others by leave-one-out cross-validation. The classification accuracy findings for separation of neurodegenerative disorders were 77.5% for Alzheimer's disease vs others, 97.5% for semantic dementia vs others, 87.5% for progressive non-fluent aphasia vs others and 82.5% for behavioral variant frontotemporal dementia vs others. Data suggest that combination of intrinsic functional connectivity, glucose metabolism, and grey matter volume based on network degeneration hypothesis can serve as a valid biomarker to separate patients with distinct neurodegenerative disorders.

Zusammenfassung

Die simultane Messung intrinsischer funktioneller Konnektivität und lokaler metabolischer Aktivität mittels eines Hybrid-PET/MRT-Scanners liefert einen besseren Einblick in die Pathogenese und Diagnostik neurodegenerativer Erkrankungen wie z.B. der Demenz vom Alzheimer Typ oder der frontotemporalen Demenz in vivo. Diese These wurde mittels zwei Projekten bestätigt.

Im ersten Projekt wurde der Zusammenhang zwischen intrinsischer funktioneller Konnektivität, lokalem Glukosemetabolismus und dem Volumen der grauen Substanz im Hippocampus und Precuneus in 40 Patienten mit Alzheimer-Demenz, 21 Patienten mit Leichte kognitive Beeinträchtigung und 26 gesunden Kontrollprobanden untersucht. Der lokale Glukosemetabolismus wurde mittels 18F-fluordesoxyglocose-PET erhoben, die intrinsiche Konnektivität anhand einer ROI-basierten funktionellen Konnektivitätsanalyse von Ruhe-fMRT Daten. Eine strukturelle MRT-Messung bzw. eine voxel-basierte Morphometrieanalyse wurden zur Ermittlung des regionalen Gehirnvolumens durchgeführt. Die statistischen Gruppenvergleiche wurden für folgende Effekte korrigiert: Atrophie, partielle Volumeneffekte, Alter und Geschlecht. Unsere Ergebnisse zeigten, dass die Konnektivität zwischen Hippocampus und Precuneus bei Patienten reduziert war. Der Metabolismus im Precuneus war in der Patientengruppe graduelll reduziert, während er im Hippocampus unverändert war. Der entscheidende Befund war, dass bei Patienten mit Alzheimer Krankheit der hippocampale Metabolismus negativ mit der reduzierten funktionellen Konnektivität zwischen Hippocampus und Precuneus korrelierte. Diese Ergebnisse belegen zum ersten Mal eine reziproke Beziehung zwischen intra-hippocampalem Metabolismus und reduzierter extra-hippocampaler Konnektivität bei Patienten mit Alzheimer Krankheit. Dieses Ergebnis ist konsistent mit der hippocampalen Diskonnektivitätshypothese der Alzheimer Krankheit.

Projekt 2: Kürzlich wurde gezeigt, dass einzelne neurodegenerative Erkrankungen spezifische Hirnnetzwerke in besonderem Maße betreffen. Darauf aufbauend, testeten wir die Hypothese, dass mithilfe der Netzwerk-Degenerations-Hypothese einzelne Patienten mit Demenzen vom Alzheimer Typ und drei Subtypen der frontotemporalen Demenz (semantische Demenz, primär progressive Aphasie, frontotemporale Verlaufsform mit führender Wesensänderung)

voneinander abgegrenzt werden können. Dazu wurden im hypbrid-PET/MR-Scanner simultane 18F-fluordesoxyglocose-PET, Ruhe-fMRT und strukturelle MRT Aufnahmen von 40 Patienten gemacht. Im Anschluss, erhoben wir innerhalb der Kernregionen von vier intrinsischen Netzwerken, die gemäß der Netzwerk-Degenerations-Hypothese primär bei den zuvor beschriebenen Subtypen der Demenz betroffen sind, die sogenannte „degree centrality“ als voxel-weises Maß für die intrinsische funktionelle Konnektivität, den regionalen Glukosemetabolismus als Maß für neuronale Aktivität und voxel-based morphometry-Werte als Maß für das regionale Volumen der grauen Substanz. Nachfolgend wurde eine „support vector machine“ verwendet, um die Patienten mit Hilfe der „leave-one-out“ Kreuzvalidierung zu klassifizieren. Die Genauigkeit der Klassifizierung, wonach die Probanden korrekterweise der jeweiligen neurodegenerativen Erkrankung zugeordnet wurden, lag für die Alzheimer-Demenz bei 77,5%, für die semantische Demenz bei 97,5%, für die primär progressive Aphasie bei 87,5% und für die frontotemporale Verlaufsform mit führender Wesensänderung bei 82,5%. Unsere Daten implizieren, dass die Kombination von intrinsischer funktioneller Konnektivität, Glucosemetabolismus und Hirnvolumen wertvolle Biomarker liefern könnte, um Subtypen der Demenz basierend auf der neurodegenerative Erkrankungen spezifische valide voneinander trennen zu können.

1. GENERAL INTRODUCTION

1.1. Motivation and goal of the current thesis

Neurodegenerative disorders, including Alzheimer's disease (AD) and other forms such as frontotemporal lobar degeneration (FTLD) increasingly represent a major public health problem, thus, they have moved into the focus of research during the last 3 decades [1, 2]. However, the precise mechanisms underlying the pathogenesis of these disorders are not completely understood. Multimodal neuroimaging (e.g. PET/MRI) opens a unique opportunity to evaluate different functional, molecular and neurochemical processes in the living brain simultaneously and to study their interaction in vivo. The main focus of the current thesis is the simultaneous evaluation of resting-state functional magnetic resonance imaging (rs-fMRI), structural MRI (sMRI) and 18-Fluorodeoxyglucose positron emission tomography (FDG-PET) by use of the new hybrid PET/MRI scanner in patients with AD and FTLD which are among the most frequent forms of dementia, particularly of early age onset dementia. AD and FTLD will be compared across modalities and also against healthy subjects.

At the beginning of the current thesis, the definition, epidemiology, clinical presentation and neuropathology of AD and FTLD will be presented in details. In the next part of the introduction, methodological concepts of rs-fMRI and FDG-PET will be described, and finally, clinical applications of these modern neuroimaging techniques in AD and FTLD will be summarized. The following chapters will include the methods, results, and discussions of two separate projects. In the first project, an association between the metabolic and structural changes of hippocampus (HP)/precuneus and functional connectivity between them on 40 patients with AD, 21 patients with MCI and 26 healthy subjects will be presented. The second project is focused on a separation of distinct neurodegenerative disorders based on the "network degeneration hypothesis" using a support vector machine classification method in 20 patients with AD and 20 patients with FTLD.

1.2. Description of neurodegenerative disorders

1.2.1. Dementia

1.2.1.1. Definition

Dementia (taken from the Latin words: *de-* means "without" and *mens-* means "mind") is an umbrella term for a symptomatic appearance of cognitive decline leading to impairment in activities of daily living. Dementia describes a variety of diseases including AD, FTLD, dementia with Lewy bodies, Huntington's disease, normal pressure hydrocephalus, Creutzfeldt - Jakob disease (CJD), Wernicke-Korsakoff syndrome and vascular dementia. For a clinical diagnosis of dementia, patients are required to show a wide range of cognitive impairments, beyond what might be expected from normal aging, at least for six months. In the Diagnostic and Statistical Manual of Mental Disorders-Fifth Edition (DSM-V) (published in May 2013), the term dementia has been replaced by "neurocognitive disorders" with various degrees of severity and incorporated into the diagnostic category of "major neurocognitive disorder" [2]. For a diagnosis of dementia based on the DSM-IV criteria: a) Symptoms must include impairment in memory and also in one of the following cognitive abilities:

- Speaking coherently or understanding spoken or written sentences
- Recognizing and identifying objects to test intact sensory function
- Performing intact sensory and motor activities and comprehension of the specific required task
- Abstract thinking ability, sound judgments, and performing complex tasks

b) Cognitive disabilities must be interfering with daily life of patients [3, 4].

Based on the etiology, dementia can be classified as reversible (10-20% of cases) or irreversible disease (80-90% of cases). Common causes of potentially reversible dementia are major depression, delirium, thyroid diseases, specific vitamin deficiencies, alcohol dependency and side effects of medications. However, in the majority of cases, dementia is caused by

neurodegenerative disorders like AD, which cause neural loss in the brain that is typically irreversible [2, 4].

1.2.1.2. Epidemiology

Prevalence of dementia in 2010 was estimated at 35.6 million world-wide, meaning that it affects 5% of the population older than 65 years and 20–40% of people older than 85. Although dementia is more common in elderly, it occurs before the age of 65 (i.e. early onset dementia) [5].

1.2.2. AD

1.2.2.1. Definition

More than 100 years ago, clinical manifestations of AD was first described by a German psychiatrist, Alois Alzheimer [6]. Alzheimer's disease is a type of dementia that causes memory, thinking and behavior decline and accounts for 50 to 80 percent of dementia patients (www.alz.org)**.** DSM-IV criteria for diagnosis of AD include (i) the gradual onset and continuing decline from a previously higher level, resulting in impairment of social and occupational function; (ii) impairments in memory and one other cognitive domain such as language, word-finding difficulties, disturbance of praxis, disturbances of visual processing, visual agnosia, constructional disturbances, disturbances in executive functioning, including abstract reasoning and concentration; (iii) cognitive deficits are not due to any other psychiatric disease, neurological diseases, or systemic disease; (iv) cognitive deficits do not occur exclusively in the setting of delirium[3]. Beside DSM-IV, there is a recent version of NINCDS-ADRDA criteria to classify individuals with dementia caused specifically by AD into 3 distinct groups: *(i) Probable AD dementia:* when the criteria for dementia are met (i.e. memory, thinking and behavioral symptoms that disrupt daily life functions of patient) and information from neuroimaging or CSF biomarkers is unavailable/uninformative or positive. For a probable AD diagnosis, evidence of

either amyloid deposition (detected on PET or CSF) or neuronal injury (CSF tau, FDG-PET, or structural MRI) can be considered to be a higher level of certainty. *(ii) Possible AD dementia:* when patients present an atypical clinical course but have both types of biomarkers (i.e. amyloid deposition and neuronal injury). *(iii) Dementia unlikely due to Alzheimer's disease:* when patients do not exhibit clinical syndrome for AD dementia or regardless of meeting clinical criteria, there is another alternative diagnosis or both biomarkers for amyloid deposition and neuronal injury are negative [7]. Differential diagnosis between probable AD and other forms of dementia is usually made with psychiatric interview using behavioral and memory tests, followed by a brain scan. However, the gold standard of diagnosis is still the histopathology of brain tissue. The association between clinical symptoms, brain pathology, senile plaques and neurofibrillary tangles has been studied during the last 35 years. However, the precise etiology that triggers the development of AD still remains unknown [2].

1.2.2.2. Epidemiology

AD is the most frequent form of neurodegenerative disorders and the most frequent cause of dementia. The number of patients with AD is growing dramatically during the last decades. The current estimated prevalence in the United States is 5.2 million while 5.0 million of who are older than 65 years. Researchers are expecting that the number of patients suffering from AD may reach 115 million by 2050 due to the aging of the population [8].

Moreover, AD is one of the most costly diseases in developed countries (total payments for 2013 in US are estimated around $203 billion dollars). The average Medicaid cost for a patient older than 65 with AD and other dementias was 19 times higher than beneficiaries for a patient older than 65 but without AD and other dementias in 2008 [2]. In addition to the treatment costs of AD, these patients have problems in orientation, judgment, social behavior and communication within their environment. Thus, family members have to assist in managing these problems. All of the behavioral changes of patients have a huge impact on family caregivers. A recent study found that patients with AD and dementia need intensive daily support by family caregivers

(average of 9 hours/day) which makes different challenges for family members including chronic stress, depression, impaired immune system and decrease of income [9]. The estimated economic cost of care, provided by 15.4 million family members and other unpaid caregivers, was $216.4 billion in 2012 in the U.S.A [9].

1.2.2.3. Risk factors

Beside age as the most important risk factor of AD [2], several recent studies reported other risk factors for developing AD:

(i) Gender: AD and other forms of dementia are more frequently diagnosed in women than in men. Almost two-thirds of American patients with AD and other dementias are women due to the fact that women live longer than men on average rather than any specific sex differences in the pathogenesis of disease [10].

(II) Education: individuals with less education are at higher risk for AD and other dementias compared to subjects with more years of education. The "Cognitive reserve" theory assumes that more years of education can help individuals to compensate for the pathological changes that could induce dementia symptoms [11, 12].

(III) Ethnicity: There are ethnic differences among patients. Most of patients with AD and other dementias are non-Hispanic whites. However, African-Americans and Hispanics are more likely than white people to have AD and other dementias [13]. This difference across ethnic groups appears to be caused by non-genetic factors. High blood pressure, diabetes mellitus as well as lower level socioeconomic and education in African-Americans and Hispanic people may increase the risk of dementia [14].

(IV) Family history: individuals who have more than one first-degree relative with AD have a higher risk of developing the disease [15].

(V) Genetics: Another risk factor of AD is the apoplipoprotein E4 (APOE) gene, which is a class of apolipoprotein produced by astrocytes that transports cholesterol to neurons via ApoE

receptors. The ε4 allele of APOE has increased the risk of developing AD and has decreased the mean age of onset for AD [16].

(VI) Mild cognitive impairment (MCI): MCI is a transient period between normality and clinical dementia, and it can be considered as a synonym of incipient dementia. It has been demonstrated that a high percentage of patients with MCI will develop AD and dementia in future. However, MCI does not always lead to dementia, and in many cases, it remains stable [17].

(VII) Cardiovascular disease risk factors: Several risk factors of cardiovascular disease are also associated with a higher risk of developing AD and other dementias including smoking, diabetes mellitus, obesity, hypertension and hypercholesterolemia in the middle age population [18].

(VIII) Traumatic brain injury: Abnormal brain functions caused by injury to the head increases the risk of developing AD and other dementias by 4.5 times, in comparison with people with no head injury. For example, moderate brain injury is associated with a double risk and severe injury is associated with a 4.5 times greater risk of developing AD [19].

1.2.2.4. Clinical presentations

The progression of AD is usually very gradual and the preclinical stage of AD can take years or decades, which complicates making a definitive diagnosis because there might be a long asymptomatic period before the clinical presentation of AD. The new AD criteria and guidelines proposed three stages of AD: preclinical AD, MCI due to AD, and dementia due to AD [7]. Recent longitudinal studies demonstrated that a clinical diagnosis of MCI is an important risk factor for development of AD, as mentioned in the previous section. The rate of conversion from MCI to AD is 12% per year while the diagnosis rate is 1–2% per year for cognitively normal elderly individuals. Around 80% of patients with MCI will be converted to AD-dementia within 5 years [17]. The common symptom pattern of AD starts with the slow progression of disability in encoding and remembering new information. In general, symptoms of AD include memory loss which impairs daily life, challenges in planning and problem solving, trouble in completing

familiar practice at home or at work, time or place confusion, problems in understanding visual or spatial images, new difficulties with words in speaking or writing, misplacing things and disability to retrace steps, poor judgment, withdrawal from social activities or work and changes in mood and personality (For more information about the symptoms of AD, visit www.alz.org/10signs). The life expectancy after diagnosis is about 7 years on average and less than three percent of patients live more than 14 years after a confirmation of the diagnosis. Common cause of death is typically external factors such as infection of bed ulcers, pneumonia or urinary infections [20].

1.2.2.5. Etiology

The histopathology of AD was first described with the amyloid-plaques and the neurofibrillary tangle (NFT) in the brain. Still today, the extracellular amyloid plaques and the intracellular NFT are neuropathological hallmarks of AD. Amyloid plaques consist of the amyloid-beta peptide (Aβ) and NFTs consist of the tau proteins [2]. The amyloid-hypothesis suggests that Aβ proteins are the main initiators of AD pathogenesis, while the tau-hypothesis focuses on the role of tau to precede the development of AD.

Amyloid model: The Aβ proteins are cleaved from the amyloid precursor protein (APP) and aggregate extracellularly to make several flexible soluble oligomers in different forms. The $A\beta_{40}$ is the most common form and $A\beta_{42}$ is the fibrillogenic form that is associated with AD. Thus, mutations in APP may imbalance the production of $A\beta_{40\ and}$ $A\beta_{42}$ and increase the relative production of $A\beta_{42}$ [21]. It has been suggested that the soluble amyloid-beta oligomers represent the most toxic form of amyloid because they inhibit long-term potentiation (LTP), increase long-term depression (LTD) and decrease dendritic spine density in hippocampus. However, insoluble amyloid plaques do not impair LTP that indicates that plaques are mainly inactive, but sequester Aβ peptides are synaptotoxic [22].

The amyloid hypothesis, which was raised in 1991, suggests that extracellular beta-amyloid aggregates are the most important neuropathological cause for the development of AD [23]. The

"amyloid cascade hypothesis" suggests specific sequences of pathogenic events leading to AD: First of all, mutations in APP and Presenilin 1, Presenilin 2 may increase Aß 42 production and accumulation, then oligomerization and deposition of Aß 42 may lead to progressive synaptic dysfunction. As a consequence, ionic homeostasis is altered and oxidative injury induces disruption in kinase/phosphatase activity, which accelerates construction of intracellular NFT, neural dysfunction and cell death [24]. Thus, trans-membrane proteins such as APP and PSEN1, PSEN2 have been suggested to play an important role in creating beta-amyloid deposits and in the development of AD.

Tau model: The hyperphosphorylated microtubule-associated tau proteins form NFT inside neurons, leading to the disintegration of microtubules, collapsing the transport system and finally causing cell death. Thus, there is a significant association between NFTs with neuronal loss in AD [25]. It has been discussed that tau pathology is presented before amyloid pathology in the medial temporal lobe (MTL) (particularly in the entorhinal cortex and CA1) of cognitively normal middle-age individuals, and diffuses into the neocortex in dementia. In detail, NFT first accumulated in the entorhinal cortex and locus coeruleus in stages I and II (present in more than 70% of subjects over 50 years old), then in the hippocampal CA1 and limbic system during stage III-IV, in the temporal cortex in stage V, and finally spread into the cortical regions in stage V-VI (around 25% of subjects over 80) [26]. Therefore, it has been suggested that neurofibrillary pathology in the entorhinal cortex and the locus coeruleus appears at the beginning of AD before the amyloid pathology [27]. Although tau pathology develops very slowly in cognitively normal people without amyloid pathology, the accumulation were increased significantly in individuals with simultaneous tau and Aβ pathology [28]. It has been demonstrated that neuronal loss and dementia in AD correlates mostly with the presence of "neuritic plaques" in brains which contain both tau and amyloid pathology, but neither NFT, nor amyloid alone [29]. This indicates that the presence and interaction between Aβ and tau is necessary for pathogenesis of AD [27].

Genetics: Autosomal dominant mutations only affect 1% of all AD patients and usually have an onset before the age of 65. The study of the gene encoding tau (MAPT) and genes regulating Aβ production including APP and PSEN1, PSEN2 demonstrated new insight into the neuropathology of AD. More specifically, APP, PSEN1, and PSEN2 genes have been considered

as autosomal dominant causes of AD. Mutations in APP, PSEN1 and PSEN2 increased the production of Aβ 42, which is the main component of amyloid plaques, supporting the idea that Aβ protein may trigger tau pathology [16]. A genetic study provides evidences that Aβ 42 could be an initiator of tau pathology in development of AD [30]. In addition, most patients with AD do not show autosomal-dominant inheritance and are categorized as sporadic AD. The major genetic risk factor for sporadic AD is the APOE4 allele, which can be presented in 40-80% patients and increases the risk of AD by 3 times in heterozygotes and by 15 times in homozygotes [31]. APOE4 is associated with pathogenic changes in CSF Aβ 42 protein but not with the tau protein in cognitively normal elderly individuals [2, 27].

1.2.3. FTLD

1.2.3.1. Definition

Frontotemporal lobar degeneration (FTLD) is a neurodegenerative syndrome consisting of uncommon disorders, which are generally associated with a progressive decline in personality, behavior and language. FTLD is often associated with atrophy in the frontal and temporal lobes with sparing the parietal and occipital lobes and sometimes also including degeneration of subcortical brain regions [32]. FTLD includes several subtypes: the frontal-variant or behavioral-variant (bvFTD); the progressive nonfluent aphasia (PNFA); and the semantic dementia (SD). In 1892, Arnold Pick described the first patient with the behavioral changes, aphasia, and dementia as well as focal atrophies in the left temporal and frontal lobes rather than the diffuse brain atrophy. Subsequently, the term "Pick's disease" was suggested by his pupil (*Gans 1923*) for the patients with lobar cortical atrophy. Later, pathologists suggested to use the term “FTLD” and to restrict the use of the term “Pick's disease” to only a disease with the pathologic finding of actual Pick's bodies, which is a very rare disease and difficult to diagnose in clinical routine [33].

1.2.3.2. Epidemiology

FTLD is the third most common cause of early-onset dementia (age below 65 years) after AD and vascular dementia and the prevalence of FTLD in epidemiological studies is varies between 2.7 (in Netherlands) to 15.1 (in Cambridge, UK) per 100,000 [32, 33]. Autopsy studies provided evidence that 5% of patients diagnosed with dementia had FTLD histopathology, but this prevalence might be underestimated due to the limited molecular methods to detect FTLD in the past [34]. Although FTLD typically affects people in the age range of 35–75 years (median age of onset is around 58 years), it doesn't vary between familial and sporadic subjects [32]. In addition, several studies reported that most patients with bvFTD and SD were males but PNFA cases were mainly females [35]. It has been demonstrated that patients with bvFTD (mean=57 years) and SD (mean=59 years) were significantly younger than patients with PNFA (mean=65 years) [36]. Moreover, the survival rate is different across subtypes; bvFTD has the shortest (median= 8.7 years from onset), PNFA shows intermediate (median=9.4 years) and SD has the longest (median=11.9 years) survival rate. In general, survival is shorter and cognitive decay is faster in FTLD in comparison with AD [35].

Many FTLD patients (especially bvFTD) present psychiatric symptoms such as anxiety, depression, bizarre behaviors and social interaction problems, and some caregivers or family members assume that the patient might fake the symptoms or act on purpose. Therefore, careful medical management and comprehensive explanation of the clinical course has been suggested to help the family a better understanding of disease and decrease the rate of stress in the family [33, 36]. On the other hand, FTLD often affects younger individuals and can severely influence their family members, especially because patients are in the main earning phase of their life. In a review, Litvan concluded that the public burden of a patient with FTD is as high as a patient with AD. Hence, early social support, enough education, and proper treatment for the caregiver may postpone the deterioration of FTD in society and improve the quality of life for patient and caregiver [37].

1.2.3.3. Risk factors: Few studies suggested that age, family history of FTLD, history of head injury and also thyroid diseases are specific risk factors of FTLD (e.g. 2.5 times increased risk of

FTLD in patients with thyroid disease). Genetic risk factors, including mutations of the Microtubule Associated Protein Tau (MAPT) gene and the Progranulin gene (GRN) are also reported in 40% patients [38].

1.2.3.4. Clinical presentation

Patients with FTLD show a wide range of behavioral, cognitive and neurological deficits, and they are usually classified into three clinical syndromes: one behavioral variant (bvFTD) and two language variants (SD and PNFA). Each of these clinical syndromes is associated with a distinct regional pattern of brain atrophy and clinical symptoms. A number of neuropsychological examinations and neuroimaging studies should be performed to confirm the diagnosis. Neary and colleagues developed a set of diagnostic criteria for FTLD in 1998 [39]. Later, the following diagnostic criteria were proposed, which can be practically used by clinicians to make a correct diagnosis:

1. Behavioral or cognitive problems should be presented by one of these symptoms:

- Early and progressive alteration in personality (such as difficulty in regulating behavior and inappropriate social activities)
- Early and progressive alteration in language skills (deficits in expression of language, naming of objects and concept of words).

2. The above deficits should cause dramatic impairment in social or occupational functions.

3. The course of disease should begin with a gradual onset followed by the development of deficits.

4. The deficits outlined in 1a or 1b should not be due to any other systemic or neurological conditions (e.g. stroke).

5. The clinical symptoms should not occur only during a delirium.

6. The symptoms are not better explained by another psychiatric diagnosis [32, 33].

Behavioral variant frontotemporal dementia: bvFTD is the most prevalent clinical presentation of FTLD, with personality changes in the early stage along with apathy or disinhibition and behavioral abnormalities and poor insight with relative maintenance of visuospatial skills. Apathy is manifested by the loss of motivation in personal affairs, hobbies, responsibilities and gradual social withdrawal, followed by the loss of awareness and concern personal hygiene, which can be misdiagnosed as major depression. Disinhibition is characterized by impulsivity or misjudgment, leading to bizarre behavior, including hurtful or insensitive actions to the others, shoplifting, traffic violations and rarely physical assault. The clinical diagnosis can be easily mistaken with other psychiatric disorders [32]. Regarding the cognitive abilities, patients with bvFTD show a decrease of insight, such as the complete denial of any problem or only small cognitive deficits (mild memory problems or word-finding difficulties) at the beginning. In later stages, some patients show dramatic alterations in their religious or political beliefs, repetitive motor behavior, idiosyncratic hoarding and collecting and changes in eating behavior. In general, the cognitive impairment is usually less severe as compared to the behavioral changes in these patients [33, 36].

Semantic Dementia: SD (or temporal-variant FTLD) is characterized by a bilateral atrophy within the middle and inferior temporal cortex, as well as fluent, anomic aphasia and behavioral changes [40]. Patients have progressive impairment in semantic and conceptual knowledge of words, objects and facts and they usually use substitute phrases such as "thing" or "that". However, speech is generally fluent suggesting that there is a conceptual difficulty rather than a language problem. Individuals with SD manifest deficits in the interpersonal and emotional processing. Moreover, patients with predominant right anterior temporal atrophy present similar symptoms as bvFTD such as emotional blunting, flat and bizarre affect, loss of empathy and obsession and rigidity about schedules. Subjects with the right anterior temporal atrophy are more rigid with specific types of compulsions, eating disorders, sleep disorders, weight loss and sexual dysfunction in comparison to patients with bvFTD [39, 40].

Progressive Nonfluent Aphasia: PNFA is a progressive neurodegenerative disorder of language expression and motor speech that is associated with atrophy of the left hemisphere. Language problems include slow, effortful speech, impaired production and comprehension of grammar and word finding difficulty. Patients typically show mild deficits in working memory and executive function, but episodic memory and visuospatial function are relatively intact. Behavioral alternations are less frequent and milder than in patients with bvFTD or SD [39, 40].

1.2.3.5. Etiology

FTLD-Tau: FTLD is a heterogeneous disorder with different pathological features. Some patients show tau- or ubiquitin- positive inclusions and some do not have any distinctive histological features. Approximately, 40% of patients with FTLD show tau inclusions including most cases of PNFA, 45% of bvFTD patients and few cases of SD. Tauopathies present with either transcortical gliosis with tau reactive rounded intraneuronal inclusions (Pick bodies) or tau positive NFT in neurons and glial cells [41]. In AD, the locus coeruleus, the entorhinal cortex, and the hippocampal formation are among the first targets of neurofibrillary tangles and subsequently the neocortex is affected [26]. However, tau inclusions often predominate in the neocortex of FTLD patients.

FTLD-TDP: In 2006, transactive response-DNA binding protein-43 (TDP-43), a ubiquitously expressed DNA/RNA binding protein, has been identified as a major component of the inclusions in variants of tau-negative FTLD (i.e. FTLD-U and FTLD-MND). Around 50% of patients with FTLD have TDP-43 inclusions, including most cases of SD and PNFA, as well as 45% of cases with bvFTD [41, 42].

FTLD- FUS: Around 7-20% of the patients with FTLD were clinically determined to have tau-negative inclusions for TDP-43 pathology resulting in the ‘atypical FTLD-U’ (aFTLD-U) label. Discovery of the fused in sarcoma (FUS) protein, a ubiquitously expressed DNA/RNA binding protein helped to classify these cases. FUS is mainly concentrated in the nucleus and less in the cytoplasm of a normal brain tissue. In FTLD, FUS protein can not move into the nucleus, leading

to FUS cytoplasmic accumulation mainly in the cortex, medulla, hippocampus, and motor cells of the spinal cord and hypoglossal nerve [41, 42].

Genetics: Mutations in the microtubule associated protein tau (MAPT) gene are associated with early onset bvFTD in 5% of cases. MAPT is a phosphoprotein presents mainly in the neurons and enhances microtubule polymerization, assortment and stabilization, initially in the axons. Tau mutations and abnormal tau aggregation disable binding to microtubules via hyperphosphorylation mechanisms, which have inhibitory outcomes in neurons and glial cells. Recently, it has been demonstrated that mutations of progranulin gene (GRN) are associated with the familial form of FTLD (5% of cases) [43].

1.3. Neuroimaging techniques

1.3.1. Resting state functional MRI

Recently, modern neuroimaging techniques play an important role in clinical routine. For instance, they help to optimize diagnostics, monitor therapy, and providing a better insight into the basic mechanisms of brain functions in vivo [44]. Quick and sufficient transport of glucose and oxygen from the cerebral blood to the neuronal cells (so-called hemodynamic response) is an essential step in providing energy supply for the cycling of neural neurotransmitters (mainly glutamate and GABA) related to the ongoing neuronal firing [45]. It has been demonstrated that oxygenated hemoglobin is diamagnetic and becomes paramagnetic during deoxygenation. Hence, deoxyhemoglobin alters the local magnetic susceptibility, resulting in magnetic field distortions and changes in the MR signal. The change in blood oxygenation level dependent (BOLD) is typical input signal used in the functional magnetic resonance imaging [46]. The quantitative neurovascular-coupling model suggests that BOLD signal is related to neuronal activity, meaning that the CBF response is a linear transformation of activity in neural cells. More specifically, the neuronal hemodynamic responses associate more with the local mean field potential than the local spiking rates. It indicates that the hemodynamic response is mainly induced by the input synaptic activity and not the output spiking activity [45, 47]. Similarly,

since 1994, it has been demonstrated that CBF and oxygen availability in the brain were significantly correlated to the electrical activity patterns in animals [48].

During the last decade, researchers assessed functional MRI in the resting brain, meaning that subjects are scanned using BOLD fMRI while positioned in the scanner in an awake state but without performing any particular task. Although spontaneous fluctuation of low-frequency BOLD signal (< 0.1 Hz) was initially considered to be noise [49], Biswal and colleagues demonstrated that after filtering respiration and heart rate signals, BOLD signals in the resting state are temporally correlated within the sensorimotor cortex. This discovery resulted in a new term in neuroscience, so called "resting state functional connectivity" [50, 51]. In a human study, Keller and colleagues demonstrate that the magnitude and spatial distribution of low-frequency fluctuation of the BOLD signal in a resting state can predict the pattern and magnitude of corticocortical-evoked potentials of cortex with intracranial electrodes. Finally, they conclude that low-frequency BOLD signal fluctuation in resting state provide an intrinsic representation of the neural functions in humans [52].

1.3.2. FDG-PET

Another common functional imaging technique is PET. The mechanism of this procedure is based on the emission of two gamma rays emanating from a tracer (i.e. Positron-emitting radionuclide) that is an analog of biologically active molecules. These gamma rays can be detected in the PET scanner to produce a three-dimensional image of the tracer concentration within the body [53]. For energy production, brain tissue consumes glucose via slow, aerobic glycolysis in the neurons and via fast anaerobic glycolysis in the astrocytes [54]. It has been demonstrated that glucose is the main source of brain energy and glucose metabolism is tightly coupled to regional neuronal function. Specifically, the energy-demanding synaptic activity of a neuron increases glucose uptake into surrounding glial cells and transfers lactate to the neurons, which acts as an energy carrier [53, 55]. Fludeoxyglucose (18F) or fluorodeoxyglucose [18F]FDG is a glucose analog with the positron-emitting radioactive isotope fluorine-18 substituted for the normal hydroxyl group at the second position of the glucose molecule.

Labeling of glucose with [18F] provides a quantitative measurement of the regional metabolism within the synaptic terminals that are in the neuron-astrocyte functional unit. After injection of ^{18}F-FDG into the blood, the tissue uptake of ^{18}F-FDG increases in the active region, which correlates with the local metabolism. Hence, the PET scanner can reconstruct three dimensional images of tissue distribution of ^{18}F-FDG. In particular, decrease of glucose uptake provides evidence of either a reduction in the number of synapses or a decline of synaptic metabolic activity [56].

1.3.3. Hybrid PET/MRI

Multimodal neuroimaging offers an opportunity to follow different functional, molecular and neurochemical processes in a living brain and to study their interaction in research, clinical and preclinical applications simultaneously. This opportunity has persuaded researchers to analyze the results obtained with different modalities on separate scanners, but this approach needs a precise coregistration of the imaging data. In addition, mental states, physiological and metabolic functions may change on time frames of minutes/hours in some conditions, including specific brain functions (e.g. Emotion, learning and memory), different diseases (e.g. Migraine, stroke) or therapeutic interventions (e.g. Antiangiogenic agents). In the early 2000s, the PET/CT technique has been introduced to allow better regional coregistration between structural and functional imaging data. Although introduction of PET/CT is a great opportunity in clinical management of patients, the soft tissue contrast is not ideal for differentiation of distinct brain tissues. For that reason, MRI is considered to be a method of choice for brain imaging because it offers high soft tissue contrast [57]. Recently, several groups tried to add the information obtained from separate PET and MRI scanners using coregistration software [58-60]. Finally, simultaneous PET and MRI acquisition for human brain studies was introduced for the first time in 2007 (Siemens Healthcare Inc.) [61]. The advantages of the integrated PET/MRI rather than PET/CT are the possibilities of performing different MRI sequences like resting-state or task fMRI, diffusion tensor imaging (DTI) and MR-spectroscopyas, as well as improving soft-tissue contrast provided by MRI. Regarding the high intra-individual variation of neuronal activities such as metabolism

and functional connectivity in neurodegenerative diseases, studying the associated cerebral processes simultaneously in a single examination in the PET/MRI scanner can be considered an extraordinary and a promising imaging option. Moreover, the PET/MRI tool also decreases the time period of imaging for patients (one examination instead of two) and MRI has no radiation exposure, unlike CT scan [62-64]. In November 2010, the world's first whole-body hybrid PET/MRI scanner was installed at the Department of Nuclear Medicine, Klinikum rechts der Isar, Technische Universität München (TUM), Munich, Germany. This scanner combines 3 Tesla MRI-technology and a high-resolution PET-scanner in one instrument and allows simultaneous acquisition of MRI- and PET- data [65, 66].

There are some technical problems in the combination of PET and MRI. For instance, MRI-based attenuation correction (AC) is still a big challenge for this instrument because the current AC methods that are available for the whole-body PET and the PET/CT are not possible with PET/MRI (i.e. there is no transmission scan with both an external radionuclide source like whole-body PET and an x-ray source like PET/CT. Additionally, bone tissues cannot be detected in MRI, while they can be detected in CT [67, 68]. On the other hand, the PET/MRI technique has several benefits, particularly in neurodegenerative diseases. For example, MRI can exclude non-neurodegenerative reasons for cognitive impairment and PET enables clinicians to find a reliable diagnosis, to make a differential diagnosis of dementia and to make a prediction of predementia stages (e.g. MCI). The PET/MRI highlights the specific patterns of regional glucose metabolism indicating a neuronal dysfunction via FDG-PET and changes in the neurotransmitter systems and finding beta-amyloid plaques via Pittsburgh compound B (PiB)-PET [57, 64, 65]. Taken together, simultaneous PET/MRI is a precise and valid neuroimaging tool which offers a unique chance to study the relationship between PET and MRI findings and to better understand the pathogenesis of multifactorial syndromes like dementia.

1.4. Neuroimaging in AD and FTLD

1.4.1. Neuroimaging in AD

1.4.1.1. Structural MRI

Structural MRI studies in AD mainly focus on atrophy or volume changes on T1-weighted MRI via voxel-based morphometry (VBM) measurements. Brain atrophy (mainly due to the synaptic, dendritic and neuronal losses) in MTL is considered as one of the early markers of neurodegeneration [69]. It has been demonstrated that the entorhinal cortex is the earliest location of atrophy and then the hippocampus, amygdala and posterior cingulate cortex will be involved [70]. The atrophy distribution in the brain is associated with the spread of neurofibrillary tangles measured at autopsy and cognitive decline in patients [26, 71]. It has been suggested that MTL atrophy is detectable in about 10% of AD cases, at least 3-5 years before the clinical symptoms manifest and it spreads across the whole brain in 6% of cases with dementia due to AD [72]. Thus, MTL atrophy becomes one of the best-established biomarkers for diagnosing prodromal AD at a pre-dementia stage [73]. Even with the visual assessment of structural MRI, clinicians can distinguish between mild AD and normal aging with a high sensitivity and specificity (about 80–85%) [72]. The distribution and the rate of brain atrophy in post-mortem studies are more strongly correlated with dementia than amyloid plaques and NFT. However, atrophy is relatively an unspecific finding and does not allow reliable prediction of AD in the preclinical stage of AD and MCI [72, 74].

Another tool to assess the structural changes involved in neurodegeneration is diffusion tensor imaging (DTI). With DTI, one can map the diffusion process of water molecules to detect the regional anatomical connectivity in vivo. Water molecule diffusion patterns can demonstrate the microscopic changes of tissue architecture in a particular disease. Particularly, AD disrupts cell membranes and increases the mean diffusivity of water and also decreases the fractional anisotropy due to loss of tract integrity in AD and MCI [4, 74, 75].

Although structural MRI is an available, non-invasive and precise method to detect specific abnormalities in neurodegenerative diseases, it has some limitations. For instance, (i) brain atrophy is not specific to AD and it can be present in normal aging and other disorders as well. (ii) structural changes can not detect molecular hallmarks of AD (i.e. amyloid plaques or NFT). (iii) MRI has several contraindications and it is not feasible for all patients [75].

1.4.1.2. Functional MRI

In the early 2000s, several fMRI studies were performed using memory tasks and researchers found a decline of hippocampal activity and an increase of prefrontal cortex activity in AD [74, 76, 77]. However, the findings for MCI are controversial depending on the stage of disease or types of tasks. Several studies found a decrease in the activity/connectivity in MTL and some demonstrated an increase in MTL activity/connectivity, particularly at early stages of disease [78-81]. In longitudinal studies, Miller and colleagues and O'Brien and colleagues suggested that hyperactivity of the hippocampus at baseline predicts a rapid cognitive decay in later stages [80, 82]. Antiepileptic medication can suppress this increased HP activity during memory tasks and improves the associated memory deficits, suggesting that the increased HP activity is a dysfunctional state and induces memory impairments in MCI [83].

Beside specific changes within the MTL, disruption of intrinsic functional connectivity (iFC) in the default mode network (DMN) has been widely shown in AD and MCI [84-86]. The DMN consists of the posterior cingulate cortex, the ventromedial prefrontal cortex, the angular gyrus and the HP. It involves the self-referential cognitive processes and deactivates during cognitively demanding tasks related to the processing of external stimuli such as memory encoding tasks [87]. Several studies revealed that FC and structural connectivity between the main regions of the posterior part of DMN (i.e. HP and precuneus) is disrupted in AD and MCI [85, 88]. Moreover, amyloid-positive healthy elderly subjects show abnormalities in the DMN's function [89-91]. Analogously, amyloid-positive healthy elderly subjects show similar alterations within the DMN as patients. Amyloid deposition is considered a hallmark of AD and shows a spatial distribution overlapping with the DMN. This indicates that disconnection within the DMN reflects specific pathological processes occurring early in AD development. These findings are also supported by studies combining different imaging modalities [87, 89]. Drzezga and colleagues found an association between the functional disconnection within the DMN, the reduced neuronal metabolism and the amyloid burden in predementia stages of AD. They demonstrated robust spatial overlaps between the connectivity disruptions and the metabolic abnormalities in patients with early AD [92].

In addition, task or resting-state fMRI has the potential to evaluate pharmacological interventions in AD. Several studies have revealed the changes in regional activation in MCI and AD between

different brain regions after acute or chronic therapy with cholinesterase inhibitors such as rivastigmine [93], galantamine [94], donepezil hydrochloride [95]. Moreover, Bokde and colleagues revealed a decrease of activation in the dorsal visual pathway after several months of treatment with galantamine, and this effect provided efficient visual processing in AD [96].

On the other hand, fMRI has several limitations. For instance, it is not possible for all patients to undergo due to the specific contraindication of MRI. Also, analysis of fMRI images is sensitive to excessive head motion which is common in severe AD patients. Finally, standardized interpretation of the results is still challenging.

1.4.1.3. FDG-PET

FDG-PET imaging has been demonstrated to be able to visualize metabolism changes, which may be one of the early signs of dementia prior the clinical symptoms and atrophy. During the last decade, a number of studies have revealed that FDG-PET can detect specific metabolic patterns along the trajectory of AD. The most consistent metabolic abnormalities have been found in the posterior cingulate cortex (PCC), the precuneus, the temporoparietal cortex and the frontal cortical regions with the sensorimotor cortex, the visual cortex and the cerebellum remaining relatively intact [55, 97, 98].

Similar to fMRI findings, there is a controversy regarding hypometabolism within the MTL and the hippocampal formation in MCI, meaning that several studies found hypometabolism [99-101] while others showed preserved metabolism in this region [102, 103]. This controversy in the literature results from different stages of patients, different measurement and analysis methods such as considering the effect of atrophy or partial volume effect, and low spatial resolution of PET images in the HP formation. It is a fact that FDG-PET data inherently contains structural information. Thus, partial volume correction can be useful to extricate FDG-data from structural atrophy [104]. For example, reduced glucose uptake in the PCC and parietal lobe has been demonstrated in mild AD, but glucose uptake in the MTL and the hippocampal formation was rather preserved in PVE-corrected images [102, 103]. Similarly, the direct assessment of metabolism and atrophy of HP and PCC showed that hypometabolism exceeded atrophy in the

PCC/precuneus. In contrast, HP exhibited atrophy and hypometabolism to a comparable degree. Therefore, it has been suggested that the excessive hypometabolism compared to the atrophy in PCC may be induced by factors such as functional disconnection or a compensatory mechanism [105-107]. In addition, Hypometabolism observed in FDG-PET has been suggested as a biomarker of neurodegeneration to predict the rate of cognitive decline progress in the APOE4 carriers and subjects who progress to AD later [101, 108]. FDG-PET also has a capacity to evaluate pharmacological and non-pharmacological interventions in clinical trials [109, 110].

The association between brain metabolism measured by FDG-PET and other biomarkers such as amyloid deposition in AD has been assessed extensively [55, 74, 92]. Rabinovici and colleagues demonstrated that although PiB and FDG have similar accuracy to distinguish between AD and FTLD, FDG is more specific and PiB is more sensitive for differential diagnosis [111]. Moreover, it has been suggested that amyloid plaques are detectable in PiB-PET earlier than hypometabolism in FDG-PET [112]. Cohen and colleagues observed a negative correlation between PiB load and FDG metabolism along with the metabolism decline in AD. They suggested that Aβ deposition could be a determinant of metabolism by induction of cellular destruction in the parietal cortex and in the precuneus, resulting in proportional decreases in local and remote synaptic metabolism in AD. However, patients with MCI show positive correlations between PiB and metabolism, without overall metabolism alteration [113]. Furthermore, Walhovd and colleagues combined MRI, FDG-PET and CSF biomarkers for diagnostic classification in AD and they concluded that the combination of structural MRI and CSF biomarkers significantly improved diagnostic classification for AD. Also, MR morphometry and FDG-PET data provided better prediction of clinical symptoms rather than CSF biomarkers alone [114]. Another study has revealed that FDG was correlated with less CSF-Aβ and high CSF-tau in clinically normal amyloid-positive older subjects [115].

In summary, glucose metabolism with [18F]FDG-PET can serve as a valid measurement for early diagnosis of AD and can help to differentiate between MCI based on early AD versus MCI based on other reasons . However, FDG is not only a relatively expensive method, but it also requires exposure to radioactivity and its spatial resolution is lower compared to MRI.

1.4.2. Neuroimaging in FTLD

1.4.2.1. Structural MRI

Some reviews and meta-analyses have shown that in the early stage of bvFTD, there is a robust atrophy in the frontal lobe (including anterior medial frontal, gyrus rectus and superior frontal, rostromedial frontal, dorsolateral frontal and orbitofrontal), anterior cingulate, anterior insula and ventral striatum and dorsomedial thalamus, particularly in the right hemisphere. In the later stages, which have a higher CDR score, atrophy extends into the frontal lobe, posterior insula, temporal and anterior parietal regions [116, 117]. The vulnerable regions including anterior insula are part of a well-known neural network, the so-called "salience network", and it has been demonstrated that frontoinsular salience network functional connectivity correlated with the severity of bvFTD [118]. On the other hand, there are some patients with clinical symptoms, but without any abnormality in the structural MRI or FDG-PET imaging indicating the 'benign' or 'nonprogressive' form of bvFTD [119-121].

In the typical variant of SD, there is significant atrophy in the left temporal lobe, particularly in the temporal pole, perirhinal cortex and anterior fusiform gyrus, hippocampus and amygdala, while the superior temporal gyrus is spared [122, 123]. During the progression of SD, the right hemisphere could be involved as well [124]. Several studies have demonstrated that evidence of atrophy is obvious in the left inferior frontal lobe, insula and premotor cortex in the early phase of PNFA [125, 126]. One case study that followed a PNFA subject for 2 years suggested the progression of clinical disruption and cortical atrophy within the language network, including the inferior frontal gyrus, temporoparietal junction, and lateral temporal cortex. However, general peak atrophy remained on the left side [127]. Similarly, Gunawardena and colleagues provided evidence that deficits with grammatical processing associated with left inferior frontal and anterior-superior temporal thinning is the probable reason for non-fluent speech in PNFA [128].

1.4.2.2. Functional MRI

fMRI studies indicated an association between the distinct patterns of a clinical FTLD syndrome with selective impairment in the large-scale networks. For example, Seeley and colleagues demonstrated that the syndromic atrophy foci anchor large-scale functional networks in the healthy subjects, meaning that the left temporal lobe (LT) of the "temporal pole-subgenual cingulate-ventral striatum-amygdala network" characterized for SD; the inferior frontal gyrus (IFG) of a network, which includes the frontal operculum, bilateral inferior parietal lobule, and primary and supplementary motor cortices, characterized for PNFA; and the right frontoinsula (RFI) of "salience network" characterized for bvFTD, with exact coordinates derived from previous studies [122]. In another study, Zhou and colleagues illustrated that bvFTD and AD trigger divergent network functional connectivity patterns. Patients with bvFTD have FC reduction in the salience network and increased FC in the DMN, however, AD showed the opposite pattern, suggesting the reciprocal network interactions. Additionally, an aberrant FC pattern in the salience network was correlated with the severity of CDR behavioral score in their study [118]. Recently, Agosta and colleagues applied graph theory analysis on the rs-fMRI of patients with bvFTD and they found altered global and local functional networks. This means that the efficiency of information exchange between brain regions might cause their clinical symptoms [129].

Recently, one fMRI case study assessed episodic autobiographical memory retrieval in two patients with SD who showed different patterns of hippocampal atrophy in comparison with a group of healthy control subjects. They concluded that the amount of hippocampal atrophy in SD alters autobiographical recollection and up-regulation of cortical areas, and FC within the autobiographical network is not able to compensate the memory impairments in patients with high degrees of hippocampal atrophy [130]. Using fMRI, Cooke and colleagues demonstrated that patients with PNFA have a lower activation of left ventral inferior frontal cortex and that this specific pattern of sentence comprehension deficit could be due to the selective disruption of a large-scale neural network contributing to sentence processing [131].

1.4.2.3. FDG-PET

In FTD, cerebral glucose metabolism is impaired in the mesial frontal cortex, anterior temporal cortices, which is distributed to other brain regions in severe cases such as caudate nuclei and the thalamus [132]. Diehl-Schmid and colleagues evaluated patients with mild bvFTD and patients with mild SD. They found two distinct patterns of glucose metabolism, meaning that patients with bvFTD had frontal hypometabolism, and patients with SD showed hypometabolism in temporal lobes [133]. In a separate work, they found that patients with bvFTD have shown a bilateral hypometabolism within the frontal lobes (not including the motor cortex), anterior cingulated gyrus, insula, caudate nuclei and thalamus. The observed hypometabolism distributed into the parietal and temporal cortices, as the disease progressed [134]. Furthermore, Drzezga and colleagues have measured amyloid plaques as well as cerebral glucose metabolism in SD and AD. They provided evidence that in AD there is a hypometabolism in the bilateral posterior cingulate, temporoparietal and frontal cortex, but in SD, the hympometabolims was restricted to the polar temporal and frontal mesial cortex. However, PiB-PET imaging with the [11C]PIB amyloid plaque tracer was observed exclusively in AD (in the bilateral temporoparietal, frontal and posterior cingulate cortex and the precuneus cortices) but not in SD [135]. In addition, patients with PNFA showed a hypometabolism in the left middle frontal, inferior temporal, angular gyri, bilateral caudate nuclei and thalamus. A negative correlation between education and glucose metabolism in the left inferior temporal, parahippocampal, and supramarginal gyri has been shown [136]. In another study, Kipps and colleagues evaluated brain metabolism and structural MRI in 24 patients with bvFTD. Their results revealed the frontotemporal hypometabolism in the mesial and orbitofrontal areas in the patients with abnormal MRI, even after correcting for atrophy, whereas brain metabolism was comparable with normal MRI and control subjects [120].

1.4.2.4. Classification

Recently, researchers tried to identify particular patterns of atrophy in FTLD to differentiate AD from FTLD or even to separate subtypes of FTLD using different characteristics of structural-MRI [137]. For instance, VBM was applied to differentiate AD from FTD using several regions

of interest. Hippocamal atrophy provided a high accuracy to differentiate between the two disorders [138]. Moreover, an association between clinical classification of FTD (with ubiquitin or tau inclusions) and particular patterns of regional atrophy rather than their histological characteristics has been shown [139]. One study provided evidence that DTI, particularly radial diffusivity, offers a better accuracy to separate FTLD subtypes than brain atrophy [140].

It has been suggested that FDG-PET can improve distinguishing FTLD and AD with 85% sensitivity and specificity [141]. A meta-analysis demonstrated that exclusive analysis of atrophy in structural MRI was not able to distinguish AD from FTLD because of a common atrophic temporal brain region in AD and SD (i.e. amygdala and hippocampus). However, by adding other imaging markers in AD, one can improve differentiation between dementias [142]. Dukart and colleagues indicated that the combined FDG-PET and MRI information using a whole-brain and region-of-interest (ROI) based support vector machine can improve the classification of patients with AD and FTLD [143, 144]. In summary, structural MRI, rs-fMRI and glucose metabolism measured with FDG-PET are valid tools to confirm the diagnosis of AD and FTLD and to explain the neurobiology of neurodegenerative disorders in vivo.

1.5. Scientific questions of the current thesis

According to the promising application of simultaneous PET/MRI in neuredegenrative disorders, I have tried to study the relationship between FDG-PET and MRI findings to better understand the pathogenesis of AD and FTLD. Thus, the following questions were formulated for the present thesis:

Project- I: The hippocampus is one of the most vulnerable regions which is targeted early in AD and several studies revealed that HP activity during memory tasks is increased in early AD while it is decreased in later stages of AD and it has been shown that increased HP activity is a dysfunctional state and induces memory impairments in MCI [76, 83]. Recently, our group found progressively increased synchrony of ongoing HP activity at resting-state along MCI and AD, which was associated with decrease of functional connectivity between HP and the neocortex as well as memory impairment [145]. These findings suggest that HP disconnection may lead to intra-HP disinhibition, expressed by increased intra-HP synchrony and activity [83, 146]. Therefore, HP disconnection from neocortical regions may contribute to increased intra-HP synchrony in patients with early AD.

Our previous study focusing on intra-HP synchronous activity opens the question whether, beyond synchrony, effective neuronal activity (i.e. metabolism) within the HP is linked with global HP disconnection. To address this question, we performed simultaneous acquisition of FDG-PET, resting-state fMRI and structural MRI in a hybrid PET/MRI scanner on patients with AD, MCI and healthy subjects in this project. We used FDG-PET activity (i.e. glucose metabolism related to glutamate-dependent neural activity) as a surrogate of effective neuronal HP activity and related it with iFC between the HP and medial parietal cortex (specifically with the precuneus) in healthy controls and patients with MCI and patients with AD. To be independent of accompanying atrophy, we also performed structural MRI and VBM analysis, and accounted for the influence of atrophy on iFC and FDG-activity. We hypothesized that a decrease of iFC between precuneus and HP is associated with an increase of metabolism within the HP in AD. To test it, we performed seed-based FC (seed: precuneus, target: bilateral HP) and then we used spatial maps of the precuneus and a one sample t-test FC of healthy subjects within the HP to analyze regional glucose metabolism and grey matter volume, which ere respectively

derived from regional FDG-PET and VBM scores in the precuneus and HP. Finally, partial correlation analyses were carried out between iFC and VBM/FDG scores using age and gender as covariates-of-no-interest.

Project- II: The network degeneration hypothesis (NDH) of neurodegenerative diseases suggests that start and propagation of pathological changes are linked with pathophysiological aspects of intrinsic network biology [147]. For example, pathology propagation seems to be linked with intrinsic connectivity of networks (wire together, die together) [118, 122]. In this project, we refer to the NDH to ask whether network specific changes measured by multimodal neuroimaging enable us to separate individuals with distinct neurodegenerative dementias.
Recently, several biomarkers have been suggested to differentiate distinct neurodegenerative disorders [142-144] but imaging-based distinction between common types of dementia is still a big challenge. We stated the question whether NDH can help to separate AD and 3 main subtypes of FTLD: namely, SD, PNFA and bvFTD. We focused on four intrinsic networks, which are hypothesized to be primarily affected by those four diseases based on NDH [122], and measured the multimodal properties of these regions including intrinsic functional connectivity (iFC), effective neural activity (metabolism), and grey matter volume. We hypothesized that multimodal properties of such cores can serve as biomarkers to differentiate individuals with distinct neurodegenerative diseases. To test this hypothesis, we used a hybrid PET/MRI scanner to assess simultaneous rs-fMRI, FDG-PET and sMRI in forty patients with dementia including 20 patients with AD and 20 patients with FTLD. Four cores from corresponding NDH-based intrinsic networks were defined from previous studies [122]. Then, for each individual patient and for each core-seeded functional network, we calculated degree centrality (DC) as the surrogate for iFC, regional glucose metabolism as the surrogate for effective neuronal activity, and VBM as the surrogate for regional gray matter volume (GMV). Afterwards, a support vector machine was used to classify individual patients with a unimodal and with multimodal approaches.

2. PROJECT- I

Association between metabolic and structural changes of the hippocampus and the precuneus with disruption of functional connectivity between them in Alzheimer's disease

2.1. BACKGROUND & HYPOTHESIS

iFC changes in AD and MCI: Disruption of intrinsic functional connectivity within the DMN has been demonstrated in AD [148-151]. In addition, MCI, a high-risk condition for AD, can also be characterized by selective changes of intrinsic neural networks in the DMN [84, 86]. Furthermore, amyloid-positive healthy elderly subjects show abnormalities in the DMN's function [89, 91]. It has been demonstrated that functional changes of neuronal networks are detectable ahead of structural changes in preclinical stages of AD [85]. Recently, iFC disruption within the DMN, particularly between the hippocampus and the retrosplenial cortex (RSC), including the posterior cingulate cortex (PCC) and the precuneus regions, has been suggested as an early neuroimaging biomarker for diagnosis of AD and MCI [84, 85, 88, 150, 151]. However, the underlying mechanism and consequences of iFC disruption within the DMN in AD and MCI is not well understood.

Local metabolic and structural changes: In Alzheimer's disease, not only functional connectivity itself within the DMN is impaired, but also several other neuropathologies associated with AD, including amyloid-deposition, tau pathology, neuronal dysfunction, and atrophy have been demonstrated to target different core regions of the DMN [91, 147]. The striking spatial overlap of these pathologies has led to the "network degeneration hypothesis", suggesting that neurodegeneration appears to spread within predefined functional networks of the brain [122]. Among the compounds of the DMN, the precuneus and the HP were identified as key regions, struck particularly strong and early in the disease course by the mentioned AD-pathologies. Both regions have been discussed to have a crucial role in memory processing. Whereas the precuneus and the PCC have critical roles in memory processing, specifically during encoding and retrieval, the HP is a key region for consolidation of information in episodic

memory processes [76]. Consequently, the impaired function of these regions will necessarily result in impaired memory performance. Interestingly, although both areas are influenced by abnormalities in early stages of disease, they appear to be affected by different forms of pathology unequally. The precuneus/PCC appears to be a highly vulnerable region to atrophy, amyloid deposition and metabolic changes [55, 91, 105-107]. Studies using FDG-PET revealed an early hypometabolism in this region in AD [55, 126, 152-154] and in MCI [55, 153, 154]. On the other hand, the HP has been demonstrated to be affected by atrophy more strongly. Several studies have discussed that the highest and earliest brain atrophy can be seen in the entorhinal and the hippocampal formation [155-157]. Similarly, amyloid-deposition has not been found to be strongly expressed in the HP compared to the other brain regions [158, 159]. However, results regarding the HP metabolism alteration have been less conclusive. Some studies detected obvious hypometabolism [99, 104, 160] and some authors found a preserved HP metabolism in AD [102, 103].

Relationship between iFC, FDG metabolism and structural changes: Recent studies have assessed the relationship between the HP and the distant regions in the posterior DMN (including the PCC/precuneus) by using different neuroimaging approaches [84, 85, 88, 105, 106, 158]. For instance, the direct assessment of metabolism and atrophy of HP and PCC showed that hypometabolism exceeded atrophy in the PCC. In contrast, the HP exhibited atrophy and hypometabolism to a comparable degree. Therefore, it was suggested that the excessive hypometabolism in the PCC relative to its atrophy may arise from the remote effect of AD-specific neuronal damage to the hippocampal formation (e.g. via functional disconnection) [105-107, 158]. Furthermore, another study using fMRI and DTI revealed that not only iFC from the PCC and the HP to the whole brain is decreased in MCI and AD, but also functional and structural connections between HP-precuneus regions are reduced [88]. Similarly, it has been shown that there is an iFC disruption between the HP and the precuneus, as well as, robust atrophy in both regions, and the correlation analyses suggested that aberrant iFC may precede cortical atrophy [85]. In addition, Drzezga and colleagues found an association between the functional disconnection of brain regions (including the PCC/precuneus), the reduced neuronal

activity and the amyloid burden in predementia stages of AD. They also showed a significant spatial overlap between connectivity disruption and hypometabolic abnormality [92].

Question and hypothesis: The main aim of this study was to understand the relationship between local changes of precuneus/HP with the disruption of functional connectivity between them in AD and MCI. Although the evidence indicates that there might be a quantitative and potentially causal interrelation between the observed regional pathologies in precuneus/HP and their functional disconnection, these interactions are not yet sufficiently understood. The question remains whether and how the local changes of precuneus/HP may associate with the aberrant iFC between them in early AD. Recently, it has been demonstrated that the progressive disconnection between HP and cortical areas is associated with the increased HP intrinsic activity in AD and these changes link with memory impairment [145]. These findings indicate that increased intrinsic activity of the HP may not represent a sufficient compensation mechanism but rather a sign of pathology itself. Supporting this notion, anti-epileptic medication has been demonstrated to normalize HP hyperactivity and at the same time improves cognitive performance in MCI patients. Moreover, anti-epileptic medications normalized the HP hyperactivity and corresponding cognitive impairments in MCI [83]. Thus, we hypothesized a negative correlation between HP glucose metabolism and iFC between the hippocampus and the precuneus in patients with early AD. To address this question, we performed the simultaneous acquisition of FDG-PET, resting-state fMRI and structural MRI in a hybrid PET/MRI scanner, which offers a unique opportunity to assess the interrelation between the structural and metabolic pathologies and their functional consequences in-vivo.

2.2. METHODS

2.2.1. Subjects

Altogether, 61 patients participated in the current study. Forty patients with mild to moderate AD-dementia (female/male: 20/20; mean age: 70.83 (SD: 8.18)) and 21 patients with MCI (female/male: 14/7; mean age: 66.81 (SD: 9.77)) were recruited (Table 1). Moreover, we used

preexisting data of 26 healthy control subjects from previous PET/MRI study (female/male: 9/17; mean age: 55.58 (SD: 10.21)) [66].

Our patients were outpatients recruited from the memory clinic of the department of psychiatry, Technische Universität München (TUM). The standard clinical/neuropsychological examination protocols as well as the integrated FDG-PET/MRI examination protocol were performed for all patients in the course of their routine clinical examination. The examination of participants included a medical history check, an interview with an informant (relative for the patients), a neurological examination and a psychometric and neuropsychological assessment [(Consortium to establish a registry for AD, CERAD battery)] [161]. Patients with MCI met the standard diagnostic criteria for [162] and had a CDR-global of 0.5, including reported and neuropsychologically assessed cognitive impairments that are not yet sufficient for a diagnosis of dementia, and they showed largely intact activities of daily life. Patients with AD-dementia fulfilled the criteria for mild dementia (CDR-global=1) and also the National Institute of Neurological and Communicative Disorders and Stroke and the Alzheimer's Disease and Related Disorders Association (NINCIDS-ADRDA) criteria for AD [7]. The exclusion criteria were any other neurological, psychiatric, systemic diseases, clinically remarkable MRI non-neurodegenerative abnormalities that could be related to cognitive impairment, a history of head injury and all MRI contraindications. None of the subjects received psychotropic medication, especially cholinesterase inhibitors at the time of scanning and no patients dropped out during the scanning session. Structural images from all subjects were inspected by a neuroradiologist to exclude any gross structural abnormalities. After receiving an approval from the local ethics committee of Technische Universität München (TUM), all the participants provided informed consent in accordance with the Human Research Committee guidelines of the Klinikum Rechts der Isar, TUM.

2.2.2. Data acquisition & preprocessing

PET/MRI instrumentation: This study was performed on a fully integrated whole body PET/MRI (Siemens Biograph mMR, Siemens Healthcare) system that consists of a PET system placed inside a state-of-the-art 3T MRI scanner. This scanner was installed in the Department of

Nuclear Medicine in November 2010 at the Technische Universität München (TUM), funded by the German Research Foundation (Deutsche Forschungsgemeinschaft) and it is operated in a collaboration between the Departments of Radiology and Nuclear Medicine of TUM and Ludwig-Maximilians-Universität (LMU). The system included a 3-T MRI scanner, features high-performance gradient systems (45 mT/m) and a slew rate of 200 T/m/s. For the cerebral acquisition, a head coil needs to be placed over the patient's cranium. To minimize attenuating influences of the radiofrequency brain surface coil and of other equipment such as patient table and cables, the latter devices were redesigned and adapted for the application in integrated PET/MRI. The integrated PET/MRI imaging is well suited for neuroimaging studies in clinical and research settings because it provides an optimal coregistration between PET and MR-data and ensures identical examination conditions. Moreover, it increases patient compliance and comfort, which is particularly advantageous in patients with neurodegenerative disorders [64, 65]. Combination of structural and functional MRI and [18F]FDG-PET, provides a unique complementary in-vivo assessment for better understanding of MCI and AD pathology.

PET/MRI Acquisition: PET-images, magnetization prepared rapid acquisition gradient echo (MP-RAGE) T1-weighted anatomical images, and T2-weighted echo-planar-imaging (EPI) MRI-data were acquired using following scanning parameters. PET: list-mode acquisition, 30 minutes after injection, 15 minutes acquisition time, 128 slices (gap 0.5mm) covering the whole brain; FoV 450mm; matrix size 192 x 192; voxel size: 3.7 x 2.3 x 2.7mm. EPI: TR/TE/a = 2.000ms/30ms/90°; 35 slices (gap 0.6mm) aligned to AC/PC covering the whole brain; FoV 192mm; matrix size 64 x 64; voxel size 3.0 x 3.0 x 3.0mm. Each measurement consists of 240 acquisitions in interleaved mode with a total scan time of 8min 08s. MP-RAGE: TR/TE/a = 2.300ms/2.98ms/9°; 160 slices (gap 0.5mm) covering the whole brain; FoV 256mm; matrix size 256 x 256; voxel size 1.0 x 1.0 x 1.0mm (for more information see [66]). Subjects were instructed to keep their eyes closed but not to fall asleep and they were questioned via intercom immediately after the resting-state fMRI scan to verify they remained awake during the scan. A medical examination of patients confirmed their stable condition before and after scanning, and nobody experienced any odd sensations during the scanning.

Preprocessing of multimodal images: We applied unified preprocessing for structural, functional MRI and PET images of each individual subject using SPM8 (Wellcome Department of Cognitive Neurology, London), in order to have all modalities in the same native space. Preprocessing of fMRI-data was adapted from previous studies [66, 163, 164]. The first three volumes of each participant resting-state fMRI scan were discarded due to magnetization effects. For each subject, realignment of fMRI images was performed. Subsequently, we coregistered intra-individual PET to the structural image and then these images to the mean-functional image. Afterwards, structural images were segmented and normalized into MNI space. The same normalization parameters were applied to fMRI and PET images. Finally, images were smoothed with a FWHM Gaussian kernel. To check data quality, temporal signal-to-noise ratio (tSNR) and point-to-point head motion were estimated for each subject to control for motion-induced artifacts [165]. In addition, extreme head motion (cumulative motion translation or rotation > 3 mm or 3° and mean point-to-point translation or rotation > 0.15 mm or 0.1°) was considered as another exclusion criterion. The absolute displacement of each brain volume compared to its previous volume was defined as the point-to-point motion. Two-sample t-tests revealed no significant differences between groups regarding average point-to-point translation or rotation of any direction ($p > 0.10$) as well as tSNR ($p > 0.50$).

2.2.3. Data analysis & Statistical analysis

Rs-fMRI data analysis: Based on our hypothesis, Volume of Interest (VOI)-based correlation was carried out on rs-fMRI data to determine voxel-wise iFC of precuneus with a previously reported protocol [163].

(i) *Subject level iFC analysis*: In order to do iFC analysis, the seed VOI was positioned on the Precuneus because it has been demonstrated that the detected BOLD time course of this seed is correlated with different brain regions in the DMN particularly with the HP [85, 166]. We used the Marsbar toolbox (http://marsbar.sourceforge.net) to create a spherical VOI (6mm radius) with center coordinates in the precuneus (3, -58, 31) based on a previous study [90] (Fig. 1 A).

After Butterworth bandpass-filtering of all the voxel time courses for the frequency range from 0.009 to 0.08 Hz, voxel time courses of seed VOI were extracted and then reduced to VOI-representative time courses by singular value decomposition. Each time course was implemented into the first-level fixed-effects general linear model in SPM8 and then iFC analysis was performed for each individual subject. For each model, global GM, white matter (WM), and cerebral spinal fluid (CSF) BOLD-signal were considered as the regressors of no-interest [163].

(ii) Group level iFC analysis: Subsequently, we performed a one-sample t-test (on the results of the first level analysis) within the healthy subjects to create the iFC map for further steps. To assess the iFC between the precuneus and the HP explicitly, a bilateral HP mask from Automated Anatomical Labeling (AAL) was created using the WFU-Pickatlas toolbox (http://fmri.wfubmc.edu/software/PickAtlas, version 2.5.2) and implemented in the model to restrict the voxel-wise precunus FC analysis to the HP region (Fig. 1 B). Afterwards, we extracted the average of all voxel iFC values within our 2 spatial maps (i.e. the precuneus and the iFC results of healthy control group in HP). Then, we performed an analysis of covariance (ANCOVA) and related least significant difference (LSD) post-hoc comparisons based on the averaged iFC values within those maps in SPSS (Statistical Package for Social Sciences, version 20). We included gender, age and GM values of HP and precuneus in SPSS analysis as covariates of no-interest.

FDG-PET data analysis: To correct FDG-PET data for a potential influence of regional cortical atrophy, we performed a correction for partial volume effects (PVE) for all subjects` scans by segmentation of each individual T1-weighted MRI in grey matter (GM), white matter (WM) and cerebrospinal fluid (CSF). An algorithm implemented in the PMOD software package (PMOD Technologies Ltd., Adliswil, Switzerland) was applied for PVE-correction as described previously [135]. We performed region of interest (hippocampus and precuneus) group comparisons using the ANCOVA and a corresponding LSD post-hoc t-test that included gender, age and GM values of precuneus and HP as covariates of no-interest with a threshold of $p<0.05$.

Structural MRI data analysis: To evaluate regional atrophy and to control for its influence on functional connectivity and metabolism results, we used the VBM8 toolbox (http://dbm.neuro.uni-jena.de/vbm.html) to analyze brain structure as described previously [164]. T1-weighted images were corrected for bias-field inhomogeneity, registered using linear (12-parameter affine) and non-linear transformations, and tissue-classified into gray matter (GM), white matter (WM), and cerebro-spinal fluid (CSF) within the same generative model [167]. The resulting GM images were modulated to account for volume changes resulting from the normalization process. In this study, we considered non-linear volume changes so that further analyses did not have to account for differences in head size. At the end, all images were smoothed with a Gaussian kernel of 8mm (FWHM). For group comparisons, ANCOVAs and related LSD post-hoc t-tests were performed for the averaged regional brain volumes restricted to regions of interest (the hippocampus and precuneus), including covariates of no-interest age and gender ($p<0.05$). Regional volumes of GM were derived from the first segmentation process and region of interests were based on results of the rs-fMRI data analysis in healthy controls as well as the precuneus seed.

Partial correlation analysis: Finally, the independent partial correlations were performed between following pairs: iFC (precuneus-HP)-FDG (HP) and iFC (precuneus-HP)-VBM (HP), FDG (HP)-VBM (HP), iFC (precuneus-HP)-FDG (precuneus), iFC (precuneus-HP)-VBM (precuneus), FDG (precuneus)-VBM (precuneus). Partial correlation represents the dependent relationship between 2 different factors controlling the influence of other factors such as age, gender and grey matter volume in the present study [168]. Therefore, we performed partial correlation across the groups including covariates of no-interest.

2.3. RESULTS

Demographic information of all participants is summarized in Table 1. Patients had significantly reduced performance scores in MMSE and CERAD scores ($p<0.05$)

Table 1. Demographic and clinical data of the participants.

	CON (n=26)	**MCI (n=21)**	**AD (n=40)**	**p-value**
Age (mean year (SD))	55.58 (10.21)	66.81 (9.77)	70.83 (8.18)	0.056
Gender (female)	9	14	20	0.109
Education (years of school)	10.10 (1.51)	10.02 (1.69)	9.84 (2.03)	0.406
MMSE (mean (SD))	29.51 (1.02)	26.93 (2.26)	22.03 (4.61)	0.000
CERAD total (mean (SD))	86.10 (8.13)	69.61 (10.44)	53.65(12.58)	0.000

ANOVA, p<0.05 as threshold of significance, except of gender (Kruskal-Wallis Test). Abbreviations: CON= healthy controls; MCI= mild cognitive impairment; AD= Alzheimer's disease; SD= standard deviation; MMSE= mini–mental state examination*; CERAD= Consortium to Establish a Registry for Alzheimer's disease.*

2.3.1. Functional connectivity changes

Group comparisons on the average of all voxel iFC values demonstrated iFC differences between three groups [F(5,86)=3.19, p=0.011]. Post-hoc t-tests revealed that iFC was altered between healthy controls and AD (p=0.003) and between controls and MCI (p=0.004) (Fig. 1 C, 3 A).

2.3.2. FDG metabolism changes

FDG-PET values were significantly different between the 3 groups for the precuneus significantly [F(5,86)=29.23, p<0.0001] but not for the HP. Post-hoc t-tests revealed a decrease in glucose metabolism in the precuneus along with AD trajectory indicating a step-wise differences between pairs of groups (CON>AD, p<0.0001), (CON>MCI, p=0.006) and (MCI >

AD, p=0.009) (Fig. 2 A, Fig. 3 B). On the other hand, FDG metabolism in HP remained unchanged across the groups (Fig. 2 B, Fig. 3 C).

2.3.3. Structural changes

The structural analysis demonstrated that the grey matter volume of the HP [$F(4,86)=12.44$, $p=0.000$] and the precuneus [$F(4,86)=6.98$, $p<0.0001$] were significantly different among all groups. Post-hoc tests revealed that for the precuneus, there were significant differences between controls and AD ($p<0.0001$) and between MCI and AD ($p=0.001$) (Fig. 2 C, Fig. 3 B). Similarly, there were differences between controls and AD ($p<0.0001$) and between MCI and AD ($p=0.006$) for the HP (Fig. 2 D, Fig. 3 C).

2.3.4. Association between functional connectivity, metabolism and structural alterations

The partial correlation analyses revealed a significant negative correlation between iFC and FDG for the hippocampus ($r= -0.301$, $p=0.032$) in AD group (Fig.4 A), suggesting that the decrease of iFC between the HP and the precuneus is associated with the increase of metabolism within the HP in AD-dementia patients. On the other hand, there was no association between iFC and FDG in the precuneus in AD ($r= -0.008$, $p=0.96$) (Fig.4 B). The positive correlations between FDG and VBM were significant for both the HP and precuneus (Fig.5 B,D) but there were no association between iFC and VBM neither for the HP, nor for the precuneus (Fig.5 A,C).

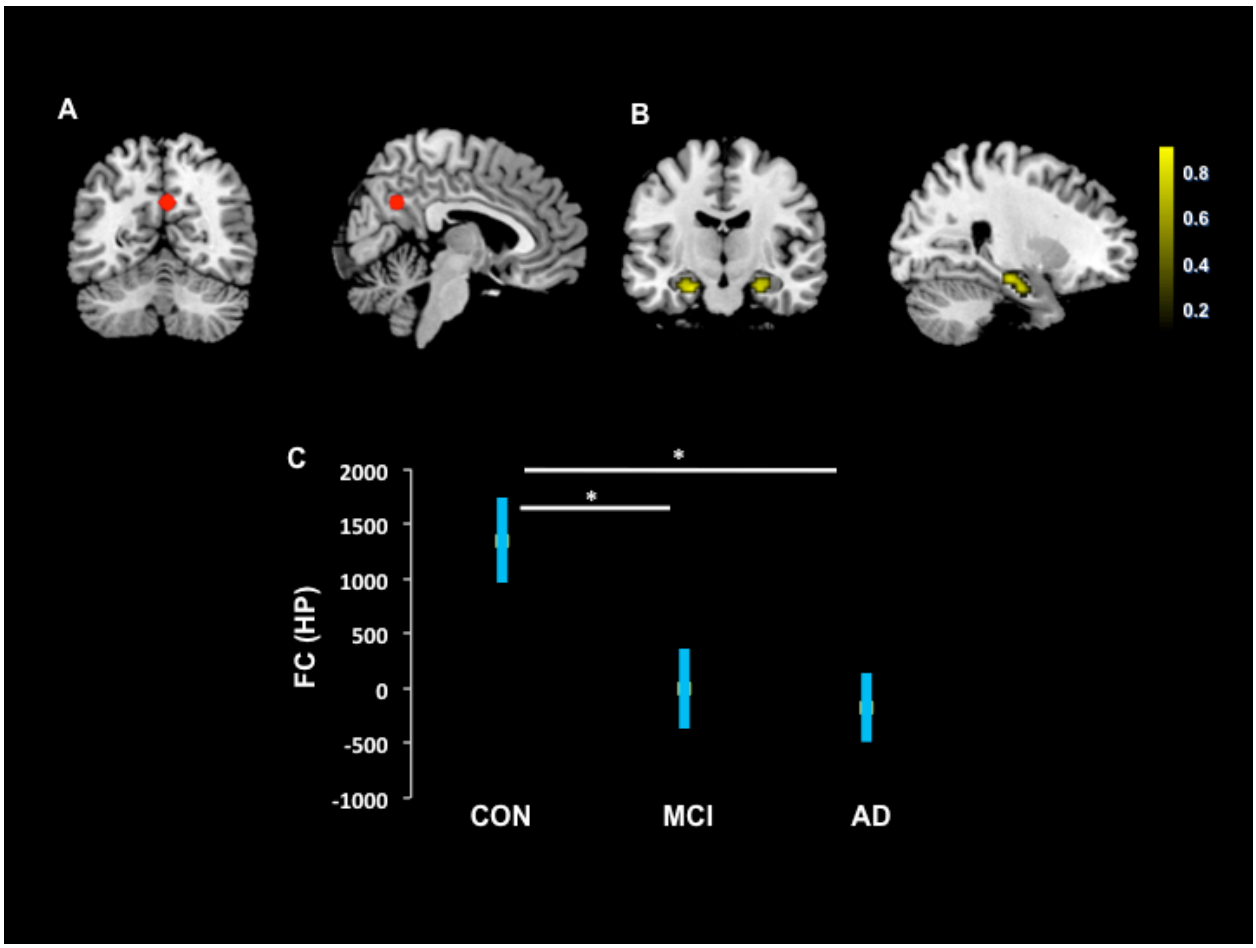

Figure 1. Regions-of-interest based resting-state functional connectivity (FC) analysis. A) The chosen ROI in the precuneus is involved in earliest stages of AD based on previous studies, and serves as seed for a seed-based FC analysis. B) The hippocampal sub-region with significant FC during rest in healthy controls (CON) serves as hippocampal ROI (one-sample t-test, $p<0.05$ FWE corrected, restricted to hippocampus mask). C) Averaged HP-precuneus functional connectivity (FC) revealed volume reductions in MCI and AD patients (ANOVA and post-hoc t-tests, $p< 0.05$).

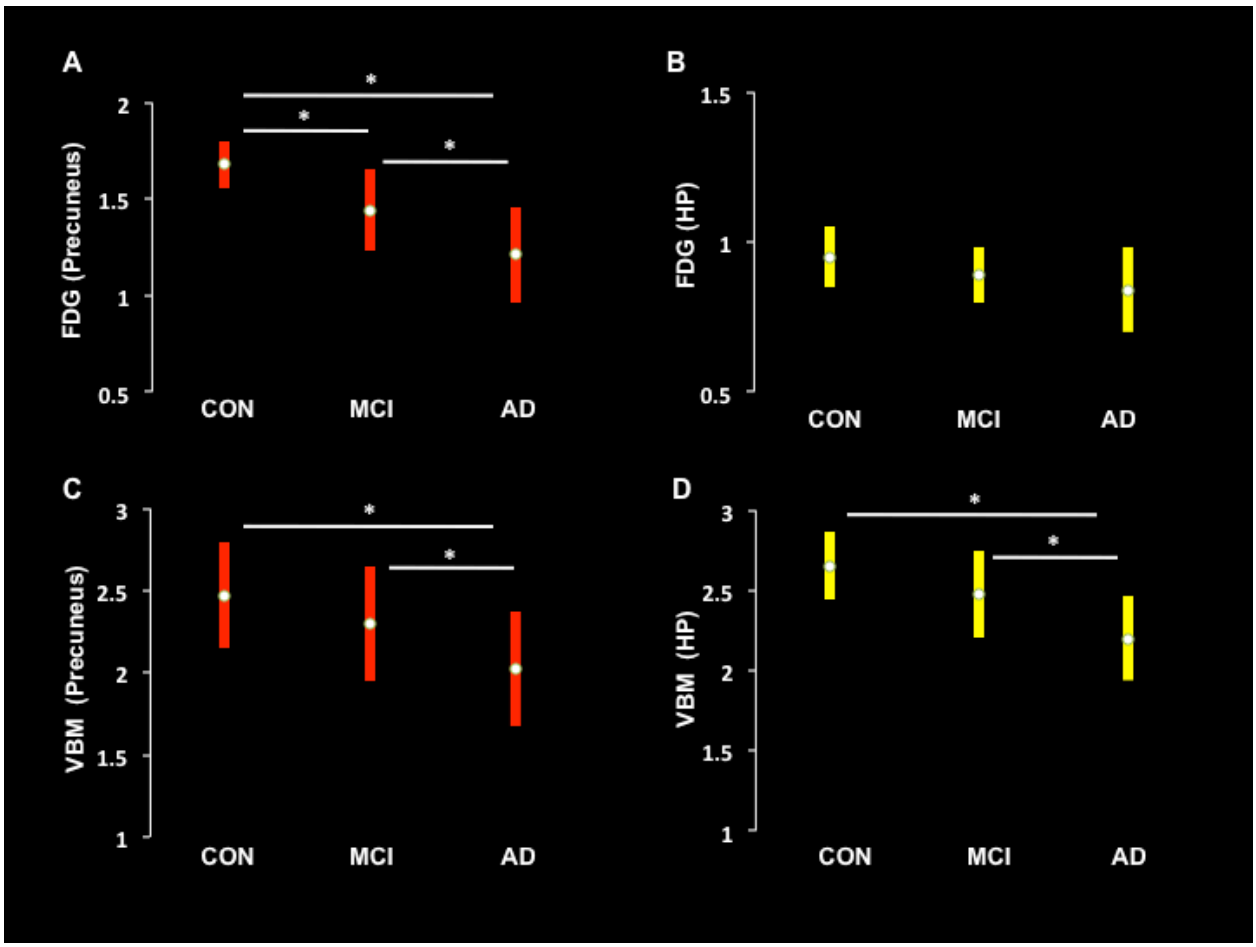

Figure 2. Regions-of-interest based glucose metabolism (FDG) and voxel-based morphometry (VBM) analysis. A) Averaged FDG values revealed reduction of glucose metabolism for precuneus in MCI and AD patients; B) Averaged FDG values revealed no changes of glucose metabolism for hippocampus (HP) across groups; C) Averaged VBM values revealed grey matter reductions for precuneus in AD patients; D) Averaged VBM values revealed grey matter reductions for HP in AD patients (ANOVA and post-hoc t-tests, $p < 0.05$).

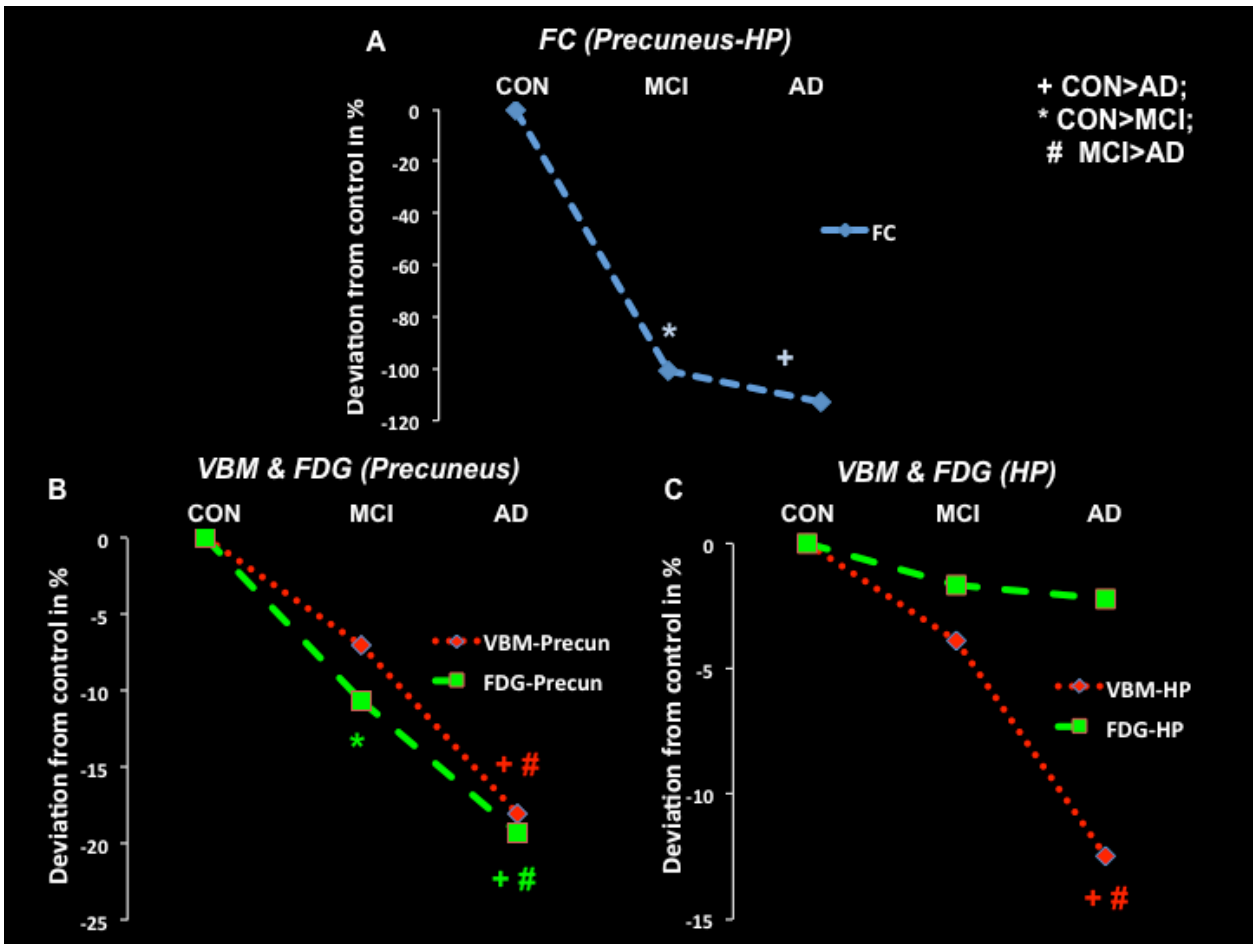

Figure 3. The patterns of functional connectivity (FC), glucose metabolism (FDG) and voxel-based morphometry (VBM) analysis. A) Reduction of FC between CON and MCI and between CON and AD; B) Reduction of both metabolism and volume in precuneus across groups; C) Reduction of HP volume but no change in HP glucose metabolism across groups (ANOVA and post-hoc t-tests, $p < 0.05$).

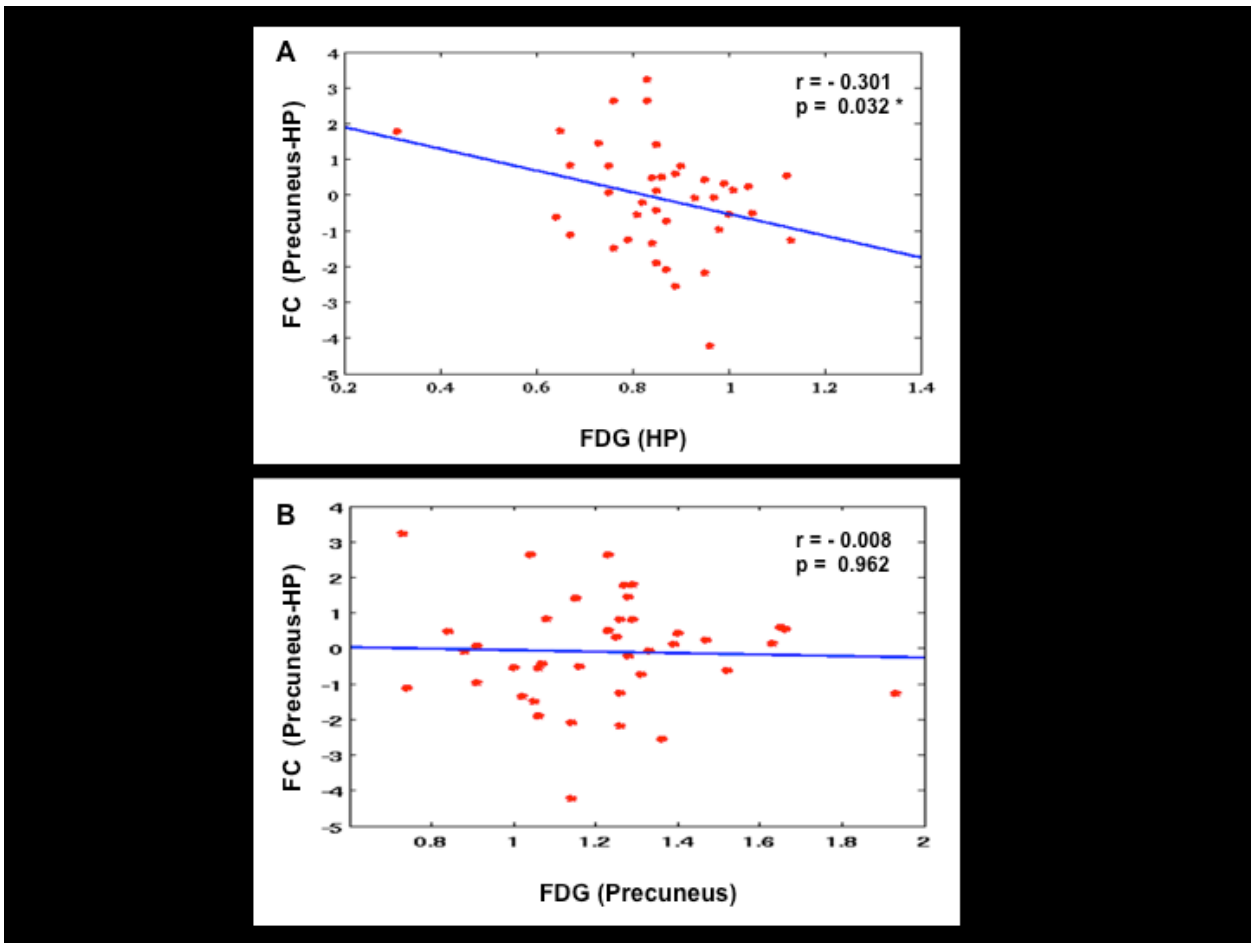

Figure 4. The relationship between functional connectivity (FC) and local glucose metabolism (FDG) for hippocampus (HP) and precuneus. A) Negatively correlated HP metabolism and precuneus-HP functional connectivity in patients with AD. B) Not correlated precuneus metabolism and precuneus-HP functional connectivity in patients with AD (partial correlation with additional variates age, gender, HP and PrC brain volume; $p<0.05$).

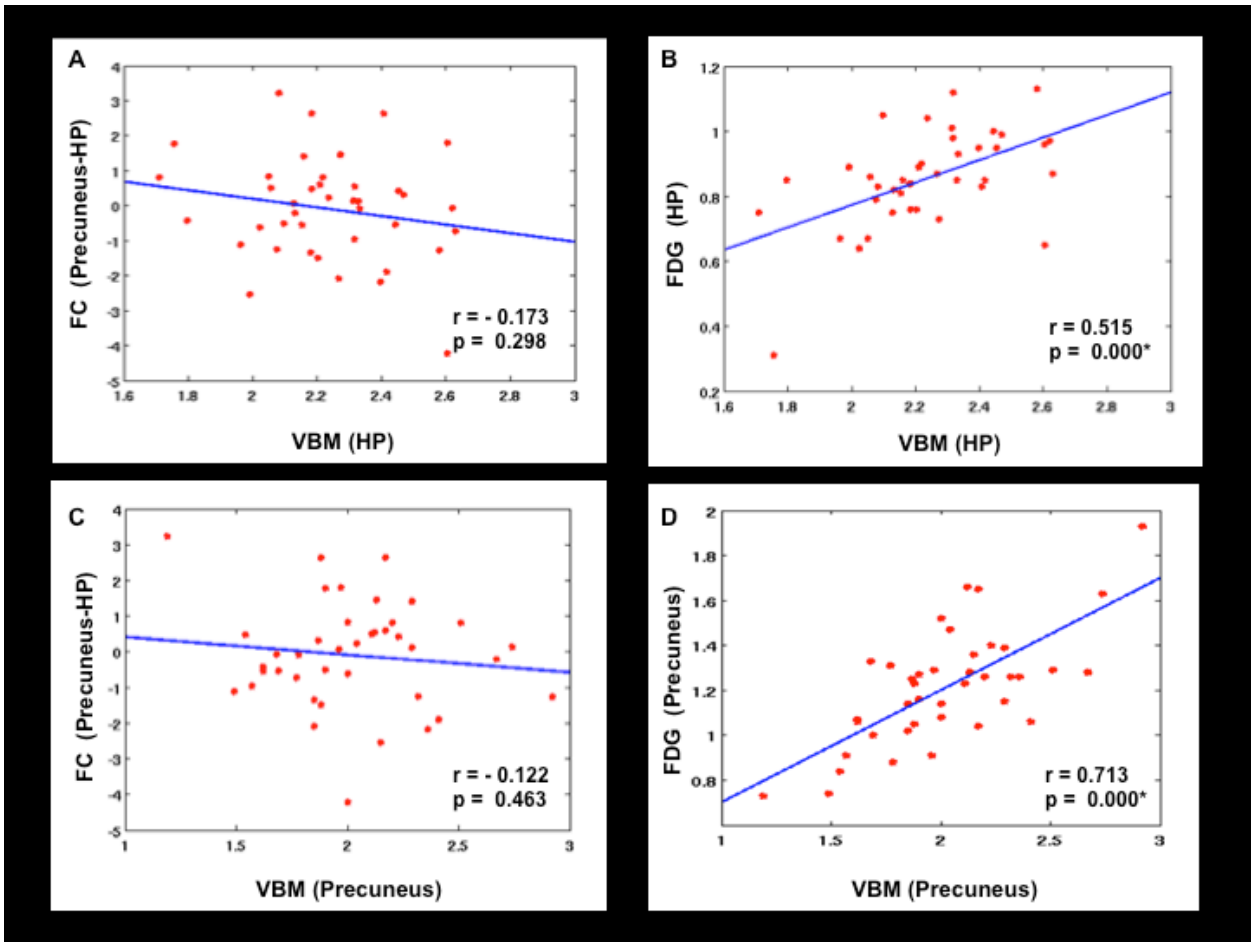

Figure 5. The relationship between functional connectivity (FC), local glucose metabolism (FDG) and voxel-based morphometry (VBM) for hippocampus (HP) and precuneus. A,C) No correlation between precuneus-HP functional connectivity and volume of HP and precunues in patients with AD. B,D) Correlated between metabolism and volume for HP and precuneus in patients with AD (partial correlation with additional covariates age, gender; $p<0.05$).

2.4. DISCUSSION

Summary of our findings: The current findings support previous studies regarding the iFC disruption between the HP and the precuneus along the trajectory of AD. Moreover, significant local atrophy and hypometabolism in the precuneus were identified along the trajectory of AD. Although, patients with AD-dementia have showed atrophy in HP but metabolism remained unchanged in HP. Interestingly, a negative correlation between iFC and HP metabolism has been found in AD, which indicates that HP metabolism may increase with the decrease of precuneus-HP functional connectivity.

Patients had reduced intrinsic connectivity between the precuneus and hippocampus: iFC findings support several previous studies regarding the reduction of iFC between the HP and precunues in the MCI and the AD groups [84-86, 88, 150]. It has been revealed that the aggregation of beta-amyloid plaques in AD may induce synaptic dysfunction [169]. Early consequences of the synaptic pathologies can be presented by disruption of functional connectivity between different brain regions, potentially occurring before the neuronal loss [86, 92, 148]. Moreover, several papers demonstrate that tau protein may be able to travel across synapses, suggesting the expansion of pathology along the connectivity pathways [170-172].

Progressive hypomebolism in the precuneus but unchanged metabolism in the hippocampus: FDG-PET findings demonstrated a significant local hypometabolism in the precuneus along the trajectory of AD but there was no significant metabolic alteration in HP among groups. Previous studies assessing metabolism and atrophy of HP and PCC revealed that hypometabolism exceeded atrophy in the PCC. In contrast, the HP exhibited a similar degree of structural and metabolic alteration [105-107]. The HP metabolic alteration is still under discussion in AD, as the detection of hypometabolism depends on the methods (e.g. partial volume correction, controlling for atrophy) and sample compositions included in the studies. Literatures on the HP metabolic changes in AD are inconsistence [99, 100, 102-104]. Samuraki and colleagues found a decline in glucose metabolism within the PCC and parietal

temporal lobe, but relatively preserved metabolism in the HP, which they interpreted to be probably due to the potential compensatory mechanisms in the hippocampus. Their results were corrected for gray matter loss and partial volume effect [102]. Our data and the results of the anti-epileptogenic medication on memory performance indicate that the change in local activity may not compensation, because MCI patients with higher intra-hippocampus activity had worse memory performance [83]. Our current findings were also controlled for confounding factors including age, gender, atrophy of both areas and also partial volume effect.

Progressively reduced grey matter volume of the precuneus and hippocampus in AD: The VBM findings support previous studies that significant atrophy differences subsist between healthy controls and AD as well as between MCI and AD-dementia for both the HP and the precuneus, Although, grey matter volume was decreased in MCI group compare to healthy subjects but the results were not significantly different. This reflects the statistical power and sample size of MCI group or it indicates that atrophy may occur relatively later in the trajectory of disease compared to iFC or FDG changes [85, 173, 174].

Association between iFC, PET, VBM: We found that the relationship between metabolism and iFC are discrepant for the HP and precuneus, meaning that the decrease of precuneus-HP iFC is associated with the increase of metabolism only within the HP in AD. No comparable relation was obvious for the precuneus. However, there was no correlation between atrophy and iFC for both the HP and the precuneus. On the basis of our findings, the following conclusions can be drawn with regard to the models of association between disrupted connectivity and regional neurodegenerative pathologies in Alzheimer-type dementia: *(i) Local grey matter atrophy of HP/precuneus may induce iFC disruption.* Our findings do not support this assumption because we observed no correlation between local grey matter values and iFC in any of our groups. Also, major atrophy was detected in the manifest AD group but not in MCI, which underlines the assumption that it may represent a late finding compared to iFC disruption and hypometabolism along the trajectory of AD. *(ii) Remote functional*

disconnection from precuneus may lead to the hypermetabolism in HP. Disruption of iFC and reduction of proper communication between the involved regions may induce disinhibition within the HP and lead to hyperactivity in the HP. This idea is in line with previous reports of increased local HP synchrony and HP disconnection in AD and MCI [145, 146, 175].

Negative association between iFC and metabolism in the HP: Our results revealed that there is a negative correlation between iFC and metabolism of HP in the AD. This means that the more functional connectivity between HP-precuneus is decreased, the more the glucose consumption in HP is increased. The perirhinal and entorhinal cortices are vulnerable regions for amyloid plaques and neurofibrillary tangles deposition in the early stages of disease, followed by the involvement of the CA1 region in the HP [26, 146, 175]. Recently, Das and colleagues provided evidence that although iFC between the medial temporal lobe (MTL) and remote hubs of the DMN is decreased, iFC between entorhinal cortex and subregions of the MTL, particularly in the anterior hippocampus is increased in MCI patients. They concluded that a dissociation of changes in iFC within the MTL compared to the changes in iFC between the MTL and other neocortical structures of the DMN can be observed [146]. Based on the previous human and animal studies, a potential underlying mechanism was suggested: an independent and synchronous increase of activity within the HP formation and adjacent regions might occur due to the decreased cortical afferents. Pathology within the enthorhinal cortex, as a vulnerable region in AD, may lead to the disinhibition of the hippocampus. This process might induce increased activity in hippocampal subsystems such as CA3/dentate gyrus [176, 177]. Yassa and colleagues used high-resolution fMRI to demonstrate hyperactivation of CA3/dentate gyrus in MCI patients during the memory task [177]. It has been demonstrated that anti-epileptics normalize hippocampus hyperactivity with simultaneous memory improvement in MCI patients, suggesting hippocampus hyperactivity as an adverse consequence of AD instead of a beneficial compensation [83]. Moreover, beyond a memory-related activity, synchrony of ongoing intra-hippocampal activity is progressively increased in MCI and AD-dementia, which is associated with the patients' memory deficits. In addition, increased local hippocampus synchrony is negatively related with progressively reduced global hippocampus iFC within the DMN [145]. Thus,

recent findings suggest that progressive hippocampus uncoupling from its main cortical input system may lead to the disinhibition of intra-hippocampal activity ("hippocampus disconnection hypothesis"). It may also be speculated that the inverse correlation between iFC and metabolism in the HP may reflect another compensatory mechanism. It has been previously discussed that the comparably well preserved metabolism in the HP-region may be a consequence of a compensatory phenomenon, i.e. that the system is trying to compensate the pathologically reduced number of synapses with a higher activity per synapse, resulting in a similar overall consumption of glucose [102].

2.5. LIMITATIONS:

The current study has several limitations. First of all, the healthy control subjects applied for this study were not aged-matched to the MCI and AD groups because we used a preexisting control-population which had been scanned on the same newly introduced integrated PET/MRI scanner and which was not exactly age-matched. Regarding the technological differences between the PET/MRI scanner and other PET-scanners (e.g. attenuation correction on the basis of MRI data etc.) [65], we decided to use this preexisting population despite the subtle age-difference. Moreover, It is clear that multimodal acquisition is problematic for subjects, we tried to avoid radiation exposure of healthy controls and preexisting control populations from other scanners could not be used in this study because of no PET and fMRI simultaneity, no multimodality, and different scanner architecture/instrumentation. Thus, we cannot exclude the possibility that some of the abnormalities detected in the group analysis between the patients and the controls are based on the difference in age rather than neurodegeneration. However, the control population in our study served rather as a common baseline to compare the extent of multimodal imaging findings between different patient groups. Our main conclusions are based on the comparison between different pathologies within the patient groups, thus they were acquired independently from the control population. Furthermore, we included age and gender of all the participants as covariates of no-interest in all analyses to eliminate their potential influence. Naturally, our results represent observational findings and do not allow any definite conclusions or a causal pathophysiological relationship.

3. PROJECT- II

Differentiation of distinct neurodegenerative disorders based on network degeneration hypothesis

3.1. BACKGROUND & HYPOTHESIS

Network degeneration hypothesis: neurodegenerative disorders in many cases result in dementia, and they are characterized by behavioral dysfunction and progressive cognitive impairment due to the increasing loss of neuronal cells and progressive neural dysfunction [178]. The clinical presentations of several neurodegenerative disorders can be distinguishable. For instance, socio-behavioral symptoms are prominent in bvFTD, while cognitive impairment is more dominant in AD [32, 118]. Recently, it has been suggested that neurodegenerative disorders do not distribute across the brain arbitrarily and they propagate via the specific intrinsic neural networks associated with cognitive-behavioral functions [116, 122, 147].

The network degeneration hypothesis (NDH) of neurodegenerative disorders suggests that the initiation and progression of pathological changes are linked with the pathophysiology of intrinsic network biology. It indicates that each neurodegenerative disorder may start in local neuronal populations and progressively distribute to the connected regions within the network ("wire together, die together") [87, 122, 147, 179]. Some proteins which are believed to be responsible for the pathogenesis of dementia, such as Aβ and tau proteins, are known to interrupt synaptic connections and axonal transport which leads to a reduction in brain network integrity [180]. Recently, it has been demonstrates that tau proteins may be able to travel across neurons, suggesting the expansion of pathology along connectivity pathways [171, 172].

Question and hypothesis: There is some evidence that AD and other neurodegenerative disorders can be considered as system level disorders. Thus, molecular, neuroimaging, or CSF biomarkers need to be evaluated with a comprehensive and large-scale view [181].

Moreover, it has been demonstrated that in memory performance, there is no significant difference between FTLD and AD patients [182]. This might result in a diagnostic doubt in clinical routine or the misdiagnosis of FTLD patients with low memory performance. Furthermore, the symptomatic appearance sometimes does not allow a reliable conclusion on the underlying causal pathology. Even dementia experts often report to misclassify dementia patients on the basis of the clinical appearance when evaluated by post mortem histopathological analysis of the brain tissue [183].

Recently, several imaging biomarkers have been suggested to differentiate various types of neurodegenerative disorders [116, 133, 142-144] but neuroimaging-based distinction between the common types of neurodegenerative disorders is still challenging. The question of the current project is whether multimodal neuroimaging can help to separate AD and three subtypes of FTLD: namely, SD, PNFA, and bvFTD, particularly when using prior regions derived from the NDH. In this study, we measured multimodal properties within the main cores of four intrinsic networks, which were shown to be primarily affected by those four disorders based on NDH [122]. Multimodal features included intrinsic functional connectivity (iFC), effective neural activity (FDG metabolism), and grey matter volume. Our hypothesis was that the multimodal properties of each core could serve as a biomarker to separate subjects with distinct neurodegenerative disorders. We focused specifically on the main core of each network, as we expected the cores to be early and most distinctly affected in neurodegenerative disorders. To address this question, we used a hybrid PET/MRI scanner to assess simultaneous rs-fMRI, FDG-PET and sMRI in 20 patients with AD and 20 patients with FTLD. Based on a previous study, we defined one core for each disorder, which had the highest atrophy for each of the four corresponding intrinsic networks [122]. Then, for all patients and for each core, the following measurements were calculated: degree centrality (DC) as a surrogate for iFC, regional glucose metabolism as a proxy for effective neuronal activity, and volumetric-based morphometry (VBM) as a surrogate for regional gray matter volume (GMV). Finally, a support vector machine (SVM) was applied to classify patients with a unimodal approach using DC, FDG, and GMV separately and with a multimodal approach using the combination of DC, FDG, and GMV.

3.2. METHODS

3.2.1. Subjects

A total number of 40 patients, including 20 outpatients with AD (male: 13; mean age: 72.2 (SD: 8.7)) and 20 outpatients with frontotemporal lobar degeneration (male: 12; mean age: 63.7 (SD: 3.9)) were recruited for this study. The FTLD patients were divided into three sub-groups, including 4 patients with SD (male: 2; mean age: 65.7 (SD: 6.0)), 5 patients with PNFA (male: 1; mean age: 68.0 (SD: 7.9)), and 11 patients with bvFTD (male: 9; mean age: 61.0 (SD: 9.6)). All participants were recruited from the memory clinic of the Department of Psychiatry, Technische Universität München (TUM). All subjects provided informed consent based on the Human Research Committee guidelines of the Klinikum rechts der Isar, TUM. We performed a standard clinical and neuropsychological assessment protocol and an integrated PET/MRI imaging protocol for each patient. Routine clinical examination of subjects included a medical history check, neurological examinations, an informant interview, including the German versions of the Bayer activities of daily living scale (BADL) [184], the Neuropsychiatric Inventory (NPI), and psychometric and neuropsychological assessments [(Consortium to establish a registry for AD, CERAD battery) [161]. Patients with AD fulfilled the criteria for mild dementia (clinical dementia rating (CDR-global=1)) and the National Institute of Neurological and Communicative Disorders and Stroke and the Alzheimer's Disease and Related Disorders Association (NINCIDS-ADRDA) criteria for AD [7]. Patients with FTLD, including SD, PNFA and bvFTD met standard diagnostic criteria for FTLD [39] and received a CDR-global of 0.5 including reported and neuropsychologically assessed cognitive impairment, not sufficient for a diagnosis of dementia and their daily life activities are undisturbed. sMRI images from all patients were evaluated by a neuroradiologist to exclude subjects with gross structural abnormalities (e.g. cerebrovascular changes or brain tumors). Other exclusion criteria were current or history of any other neurological or psychiatric disorders such as major depression, schizophrenia, alcohol or substance abuse, epilepsy, other forms of dementia, personality disorder and remarkable MRI abnormalities that could be associated with non-neurodegenerative forms of

cognitive impairment as well as all MRI contraindications. None of our patients dropped out during the study.

3.2.2. Data acquisition and preprocessing

For all participants, PET/MRI imaging was concurrently recorded by a fully-integrated whole body PET/MRI (Siemens Biograph mMR, Erlangen, Germany) system, which consists of a PET system placed inside a state-of-the-art 3T MRI scanner. We applied a unified pipeline of preprocessing to sMRI, fMRI and PET images using SPM8 (Wellcome Department of Cognitive Neurology, London). In the present study, we used non-smoothed rs-fMRI, sMRI, and FDG images for further analysis because SVM classification is typically performed without smoothing of the images [185].

3.2.3. Data analysis & Statistical analysis

Definition of cores: Based on the NDH, each of AD, SD, PNFA, and bvFTD disorders tend to develop within distinct intrinsic networks. It has been demonstrated in a previous study that the core of these networks overlaps strikingly with the peak atrophy regions in groups of patients affected by the respective disorders [122]. We selected those four cores and positioned them as follows: *(i)* at the right angular gyrus (RAng) of the "default mode network" characterized for AD; *(ii)* at the left temporal lobe (LT) of the "Temporal pole-subgenual cingulate-ventral striatum-amygdala network" characterized for SD; *(iii)* at the inferior frontal gyrus (IFG) of a network which includes the frontal operculum, primary and supplementary motor cortices, and bilateral inferior parietal lobule characterized for PNFA; *(iv)* at the right frontoinsula (RFI) of "salience network" characterized for bvFTD. We used MarsBaR (http://marsbar.sourceforge.net) to create these four spherical cores (ROIs with 10mm radius) with the exact coordinates derived from the mentioned previous study [122] including RAng (52, -58, 36, Brodmann area [BA] 39) for AD; LT (-44, 14, -25, BA 38) for SD; IFG (-43, 15, 27, BA 44/48) for PNFA RFI (35, 24, 5, BA 47) for bvFTD (Fig.6). Subsequently, iFC, VBM and FDG values were extracted within these cores for all subjects.

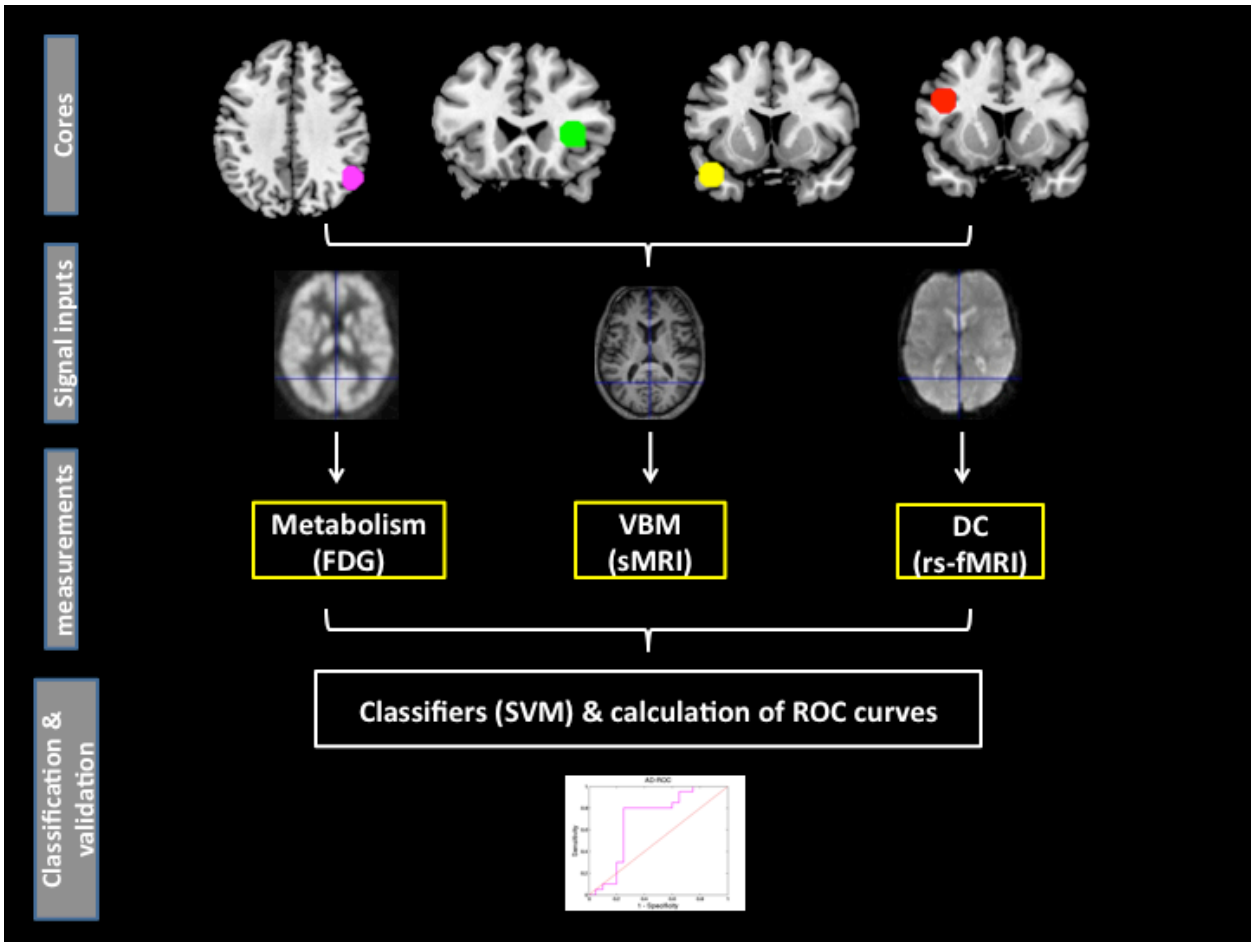

Figure 6. The protocol of analysis. The main core of each network was created based on Seeley et al. 2009. Subsequently, the voxel wise values and the averaged values of three modalities were extracted from each core for all subjects. Then, support vector machine was applied to classify each patient and finally, ROC curves were plotted.

Degree centrality as surrogate for iFC: Degree centrality reflects the sum of edges' weight that connects to a given node. Thus, nodes with high DC represent main hubs in the large-scale network [186, 187]. In other words, regions with a high DC show high functional connectivity to many other regions in the brain. Recently, several studies applied DC to examine node characteristics of intrinsic neural networks in schizophrenia [188], MDD [189], and neurodegenerative disorders [92, 129, 186, 190]. In the present study, we performed calculation of DC with the REST toolkit (http://www.restfmri.net) [191]. For each subject, a whole brain DC map was obtained by measuring the sum of Pearson's correlation coefficients between the rs-fMRI BOLD signals of the given voxel and the rest of the voxels in the brain. Subsequently, the voxel-wise DC values and the averaged DC values within the four cores (RAng, LT, IFG, RFI) were extracted for each subject. We calculated both coarse-grained level (voxel-wise) and fine-grained level (averaged values) to test the reliability of two different types of DC measurements.

FDG-PET analysis as surrogate for effective neuronal activity: To be consistent with DC, we extracted the voxel-wise and the averaged glucose uptake values within the 4 cores for each subject. Similar to DC, the voxel-wise and the averaged FDG values were extracted to control for repeatability of our measurements. The FDG-PET values were divided by the mean FDG value in the cerebellar vermis to control for interindividual variations. A cerebellar vermis ROI was created using the WFU-Pickatlas toolbox (http://fmri.wfubmc.edu/software/PickAtlas, version 2.5.2). The vermis has been suggested as one of the best-preserved disease-free areas for the scaling of PET images in neurodegenerative disorders [106]. For more details, see chapter 2.2.3.

Voxel-based morphometry as surrogate for gray matter volumes: To detect structural alterations within the four cores for each patient, we followed a VBM protocol described in a previous study [164]. For more details about VBM, see chapter 2.2.3. To be consistent with the DC and FDG analyses, the regional GMV of our cores (RAng, LT, IFG, RFI) was calculated for each individual, once for the voxel-wise GMV and once for the averaged

GMV within the cores to control for repeatability of our method.

Support Vector Machine: As described previously, the SVM procedure is performed with a linear kernel to generate a hyperplane to separate the different clinical groups of training data based on the voxel-wise or the averaged values within the four core [185]. Firstly, the information of each participant is transformed into a vector and the data of other modalities is added by extending the vector. Afterwards, leave-one-out cross-validation was applied during the training phase, where for each round of training, one subject is used for testing while the remaining data is used for training. This procedure helps to generalize the trained SVM to data that have not been presented to the SVM algorithms before. The reported classification accuracy is the percentage of cases that were assigned to the clinical diagnosis correctly [143, 192].

Classification: For each subject, as mentioned, we calculated fingerprint vectors based on three measures: DC, FDG-PET and VBM, where DC represents the intrinsic functional connectivity, FDG-PET indicates the effective neuronal activity, and VBM reflects the regional grey matter volume. To better capture the three properties, we calculated these values in both coarse-grained level (i.e. averaged value of the three properties) and fine-grained level (i.e. voxel-wise values of the three properties). Subsequently, SVM was applied to predict the status of each patient using both a unimodal and a multimodal approaches. Particularly, for all group comparisons (AD vs others, SD vs others, PNFA vs others, bvFTD vs others), the classification was performed based on DC, FDG-PET and VBM measurements, respectively. Moreover, classification was also performed on the combination three measures together. To reduce the variability of findings and evaluate the generality of an independent dataset, leave-one-out cross-validation was applied. The validity of classification was finally evaluated by the widely used measures: Accuracy, Sensitivity, Specificity and Receiver Operating Characteristic (ROC) (Fig. 6).

3.3. RESULTS

Demographic information from all subjects is summarized in Table 2.

Table 2. Demographic and clinical data of the patients

	AD (n=20)	**SD (n=4)**	**PNFA (n=5)**	**BvFTD (n=11)**	**p-value between groups**
Age (mean year (SD))	72.2 (8.7)	65.7 (6.0)	68.0 (7.9)	61.0 (9.6)	0.010
Gender (male)	13	2	1	9	0.119
MMSE (mean (SD))	22.03 (4.61)	18.75 (12.8)	18.00 (5.92)	23.73 (7.0)	0.042

AD: Alzheimer's disorder; SD: semantic dementia; PNFA: progressive nonfluent aphasia; bvFTD: behavioral variant frontotemporal dementia; MMSE: Mini–mental state examination.

For each group, the SVM classifier was applied to differentiate neurodegenerative disorders. Both the voxel-wise values and the averaged values within the four cores presented that DC, VBM and FDG and the combination of them are promising imaging biomarkers to separate distinct neurodegenerative disorders. The following accuracy *results* arose from a single modality measurement based on the voxel-wise values: *for DC*, AD vs others [70%], SD vs others [77.5%], PNFA vs others [87.5%], bvFTD vs others [70%]; *for FDG-PET*, AD vs others [72.5%], SD vs others [97.5%], PNFA vs others [85%], bvFTD vs others [60%]; *for VBM*, AD vs others [32.5%], SD vs others [92.5%], PNFA vs others [82.5%], bvFTD vs others [72.5%] (Table 3). The results for averaged-values were similar (for details, see Table 4).

Table 3. Classification accuracy based on the voxel-wise values for each core

Measurements	**Validity**	**AD vs others (AD core)**	**SD vs others (SD core)**	**PNFA vs others (PNFA core)**	**bvFTD vs others (bvFTD core)**
DC	accuracy(%)	70	77.5	87.5	70
	sensitivity(%)	55	100	0	36.3
	specificity(%)	85	75	100	82.7
FDG	accuracy(%)	72.5	97.5	85	60
	sensitivity(%)	70	100	40	36.3
	specificity(%)	75	97.2	91.2	68.9
VBM	accuracy(%)	32.5	92.5	82.5	72.5
	sensitivity(%)	35	50	0	45.4
	specificity(%)	30	97.5	94.2	82.7
DC+FDG+VBM	accuracy(%)	77.5	97.5	87.5	82.5
	sensitivity(%)	80	100	0	54.5
	specificity(%)	75	97.2	100	93.1

AD: Alzheimer's disorder; SD: semantic dementia; PNFA: progressive nonfluent aphasia; bvFTD: behavioral variant frontotemporal dementia; DC: degree centrality; FDG: Fluorodeoxyglucose*; VBM: voxel-based morphometry.*

Table 4. Classification accuracy based on the averaged values for each core

Measurements	Validity	AD vs others (AD core)	SD vs others (SD core)	PNFA vs others (PNFA core)	bvFTD vs others (bvFTD core)
DC	accuracy(%)	80	90	87.5	72.5
	sensitivity(%)	95	0	0	0
	specificity(%)	65	100	100	100
FDG	accuracy(%)	55	90	87.5	70
	sensitivity(%)	45	0	0	0
	specificity(%)	65	100	100	96
VBM	accuracy(%)	0	90	87.5	87.5
	sensitivity(%)	0	0	0	63
	specificity(%)	0	100	100	96
DC+FDG+VBM	accuracy(%)	72.5	90	87.5	72.5
	sensitivity(%)	75	0	0	09
	specificity(%)	70	1	100	96

AD: Alzheimer's disorder; SD: semantic dementia; PNFA: progressive nonfluent aphasia; bvFTD: behavioral variant frontotemporal dementia; DC: degree centrality; FDG: Fluorodeoxyglucose*; VBM: voxel-based morphometry.*

Multimodal measurements revealed that the combination of three modalities provides the best classification accuracy across the four groups based on the voxel-wise values. Particularly, classification accuracies were 77.5% for AD vs others, 97.5% for SD vs others, 87.5% for PNFA vs others, 82.5% for bvFTD vs others (Table 3). The accuracy results based on averaged values were 72.5% for AD vs others, 90% for SD vs others, 87.5% for PNFA vs

others, 72.5% for bvFTD vs others (Table4). The ROC curves on a combination of three modalities are provided in figure 3. These findings achieved the significant area under the curve (AUC) values for AD (0.69), SD (1), PNFA (0.53), and bvFTD (0.69) (Fig. 7).

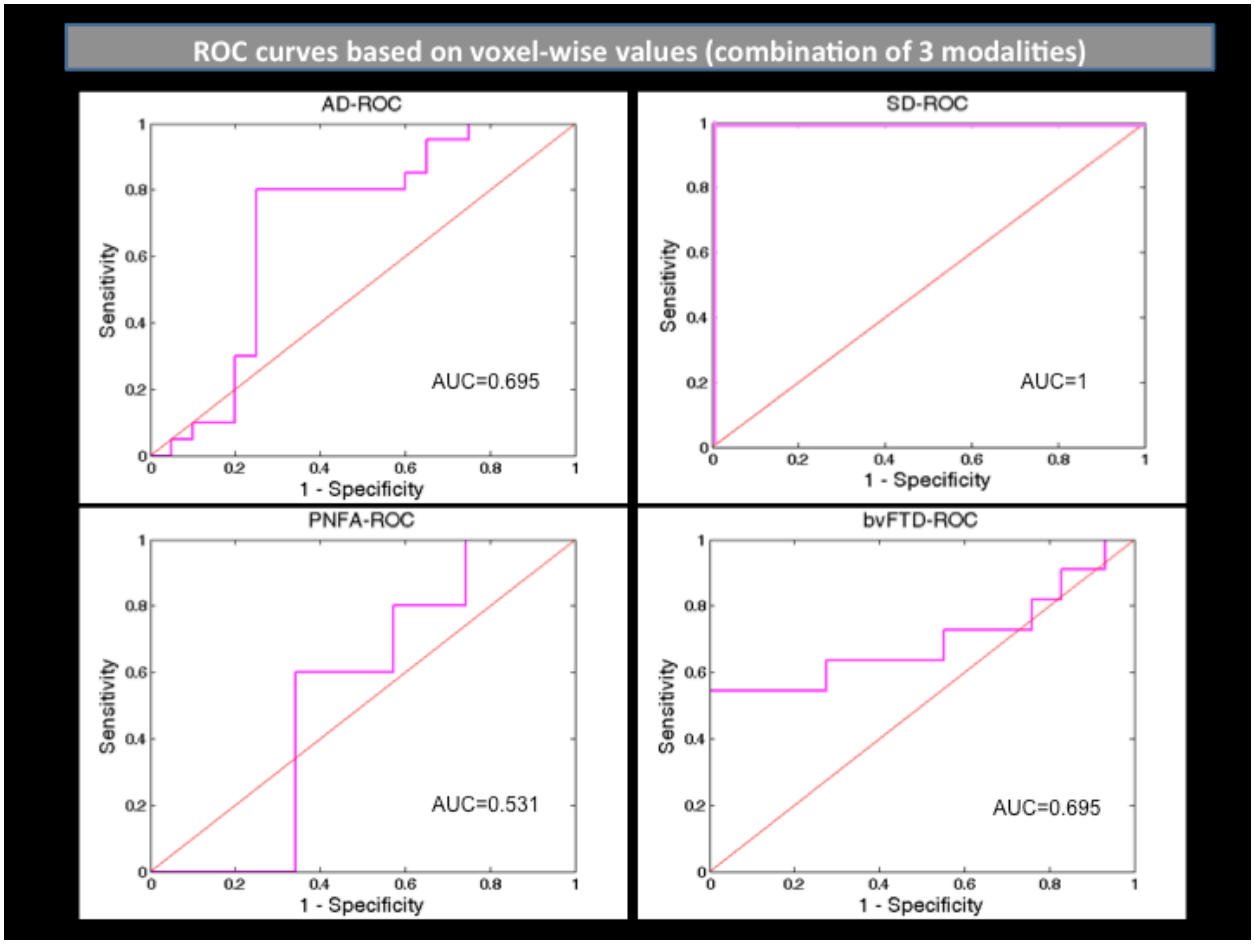

Figure 7. The Receiver Operating Characteristic curves (ROC) and area under the curves (AUC) based on multimodal voxel wise values of properties across distinct neurodegenerative disorders.

3.4. DISCUSSION

Summary of our findings: The main findings of this study are that degree centrality, grey matter volume and glucose metabolism as well as the combination of these three modalities measured in brain regions defined on the basis of assumptions derived from the NDH provide promising classification accuracy to separate AD, SD, PNFA, and bvFTD. It indicates that multimodal neuroimaging can serve as a valid biomarker to differentiate distinct neurodegenerative diseases.

The NDH suggests a new model of neurodegeneration:

Recently, growing amounts of evidence have been collected, indicating that different forms of neurodegeneration expand within different networks of the brain. For example, several studies demonstrated distinct circumscribed patterns in different early-stage dementia syndromes overlapping with specific networks of the brain [117, 193]. Moreover, amyloid-deposition has been shown to affect intrinsic brain networks [91, 92, 147] and also functional network connectivity has been demonstrated to be impaired in the corresponding networks in the respective disorders [91, 122]. Based on this model, each specific neurodegenerative disorder targets a particular brain area (i.e. starting point with the maximum abnormality) from which disease starts spreading into the large-scale intrinsic brain network. Thus, the neurodegeneration can be considered as a "disconnection syndrome" in which the functional connectivity of large-scale networks is disrupted progressively. In the other words, the NDH would explain why different patterns of neurodegeneration could be observed in the respective disorders. Furthermore, it implicates that the main core of each network (i.e. starting points) should: (i) be affected most dominantly and early in the disease process of different neurodegenerative phenomena, therefore, these regions would be ideally suited for "early diagnosis"; (ii) be affected by different pathologies including atrophy, amyloid, tau and functional connectivity changes as a cascade phenomenon; and (iii) the identification of neurodegenerative markers in the starting points specific for different forms of neurodegeneration should allow optimized "differential diagnosis".

So far, the reason(s) for this network-based expansion of disease is unclear. However, it has been suggested that particular proteins which are involve in the pathogenesis of neurodegenerative disorders, such as beta amyloid, tau, TDP-43, and alpha-synuclein, can be misfolded and aggregated within specific neural networks. Recent data demonstrates that tau poteins travel across synapses in a prion-like manner, which could explain the expansion of pathology along the connectivity pathways [171, 172].

According to this model, AD affects the ‘‘default mode network’’, which corresponds to episodic memory function; bvFTD triggers the “Salience network”, that links to emotional salience processing; SD anchors the “Temoral pole-subgenual cingulate-ventral striatum-amygdala network” responsible for semantic knowledge about words, objects and concepts; and finally, PNFA targets the “frontal operculum, primary and supplementary motor cortices, and inferior parietal lobule bilaterally” which play an important role in language and motor skills and speech fluency [118, 122, 147].

Single modality biomarkers: A valid clinical biomarker should be able to monitor disease progression and the effects of therapy in a coherent and integrated mode. Gomez-Ramirez and colleagues suggested to re-define a clinical biomarker to be a multidimensional model that can be utilized as an indicator of normal biological mechanisms, pathogenic processes, and pharmacological responses to medications. Thus, they suggested the large-scale network-based approach as a promising biomarker to detect a syndrome with multifactorial pathogenesis, such as dementia, rather than focusing on individual brain regions or specific proteins[194]). Up to now, several studies focused on single neuroimaging biomarkers or compared sensitivity and specificity of various single biomarkers to achieve the best accuracy classification [195-197].

iFC: In the present study, it was demonstrated that voxel-wise of the DC findings in the core of each network (as a surrogate for iFC) allowed classification accuracies of more than 70% across groups. The classification accuracies on our FC data are comparable with previous studies (86.6% -87%) [198]. This suggests that DC is a powerful measurement to differentiate AD, SD, PNFA, and bvFTD. Previously, it has been shown that a resting-state

functional connectivity analysis of DMN has the capacity to separate AD patients from healthy elderly subjects and MCI from normal aging. Thus, the intrinsic functional network analysis provides a potential marker to quantify the asymptomatic and prodromal stages of AD [116, 118, 199]. Similarly, functional abnormalities within the large-scale neuronal networks, including the salience, the DMN, and the fronto-parietal networks, have been shown in patients with bvFTD [200]. Zhou and colleagues revealed that AD and bvFTD exhibited divergent network connectivity patterns, indicating reciprocal network interactions. Particularly, bvFTD decreased the salience network connectivity involved in social-emotional and visceroautonomic processing, but increased the posterior DMN connectivity involved in episodic memory and visuospatial functions, and these findings were associated with the clinical severity of bvFTD. A similar analysis in AD showed opposite patterns [118]. Taken together, our results provide evidence that FC analysis based on NDH is a valid method to differentiate distinct neurodegenerative disorders.

FDG-PET: Results of the analysis of the FDG-PET data in the current study indicate that FDG can be considered to be a notable biomarker to separate AD, SD, PNFA, and bvFTD with robust classification accuracies ranging from 60%-97.5% based on voxel-wise values. Many previous studies assessed the global FDG-PET imaging or focusing on predefined target ROIs to distinguish distinct neurodegenerative disorders (for review, see [201]). Poljansky and colleagues evaluated a visual rating scale of FDG-PET images to separate FTLD from AD and MCI. They found sensitivity and specificity of 81% and 94% between FTLD and AD and 81% and 64% between FTLD and MCI, respectively. Additionally, the correct attribution of patients with FTLD to a correct diagnosis has a sensitivity of 89% [202]. In our study, we focused on the small isolated predefined cores based on NDH. However, the classification accuracies on our FDG data are comparable with the Poljansky's study. In general, our findings support the idea that FDG-PET imaging can separate neurodegenerative disorders.

VBM: Current results of structural analysis demonstrated that VBM, similar to iFC and FDG-PET provides acceptable separation accuracies between four disorders (ranging from 32.5 – 92.5). The lower classification accuracies compare to DC and FDG-PET might be due to the facts that atrophy typically appears in the advance stages of neurodegenerative disorders. Previously, Zhang and colleagues investigated regional brain atrophy and white matter microstructural changes in three subtypes of FTLD. Using diffusion tensor imaging (DTI) and VBM, they showed that each individual disease exhibited specific regional patterns of brain atrophy and white matter lesion. Although brain atrophy could separate FTLD subtypes from healthy subjects (classification accuracy ranging from 45.7%-65.7%), DTI, particularly radial diffusivity, achieved a better accuracy for FTLD classification (classification accuracy ranging from 67.6%-76%) [140]. In the present study, we did not perform DTI as our question was focused on the core of each network and not the structural connectivity between different regions. Another study compared hippocampal volumetry, tensor-based morphometry and VBM on particular regions of interest to find the best classification accuracy (72%) between AD and frontotemporal dementia. Their findings demonstrated that VBM provided the highest accuracy to classify FTD from AD [138]. In summary, our classification accuracies are comparable to the literature and our results are in the same line with previous studies in concluding that the single modality analyses using DC, FDG-PET, and VBM are valid methods to differentiate four distinct neurodegenerative disorders.

Multimodal biomarkers: The combination of three modalities in the present study obtained the best accuracy classification across our groups, ranging from 77.5% to 97.5% based on voxel-wise values. Recently, several studies have added different neuroimaging techniques to achieve a higher classification rate at discriminating neurodegenerative disorders from each other [142, 144, 185]. Frisch and colleagues tried to separate AD and FTLD using memory performance and neuroimaging techniques. They found there is no significant difference in the verbal and visual subtests from the Wechsler Memory Scale. However, using VBM and FDG-PET, they showed that memory performance is associated with the parieto-mesial cortex alteration in AD and it is correlated with changes in frontal cortical and subcortical

regions in FTLD. There was no regional overlap between AD and FTLD that was associated with memory disruption [182].

Moreover, it has been demonstrated that combining FDG-PET and structural MRI improved the detection and discrimination of AD and FTLD. For example, Schroeter and colleagues in a meta-analysis evaluated atrophy and glucose metabolism in AD (n=578) and FTLD subtypes (n=229) using conjunction analyses. They revealed that overlapping atrophy was presented only in amygdala and hippocampal head in AD and SD and there was no overlap for atrophy and metabolism changes in other regions between AD and FTLD subtypes. In additional analyses and only for AD, hypoperfusion and hypometabolism were presented in the inferior precuneus/posterior cingulate gyrus and the angular/supramarginal gyrus, indicating a regional dissociation between atrophy and hypoperfusion/hypometabolism [142]. Similarly, Dukart and colleagues combined FDG-PET and structural MRI and they found ROI-based and whole-brain SVM classifications increased detection and differentiation of AD and FTLD. Particularly, ROI-based multimodal classification provided higher classification accuracy (up to 92%) in comparison with the single modality approach to separate AD, healthy subjects, and FTLD [144]. In a meta-analysis the same group showed that SVM classification even based on multicenter data can be considered to be a valid method for diagnosis of AD [143]. In general, our findings support previous studies, mentioning the combination of different modalities such as, DC, FDG-PET, and VBM based on NDH, provides the highest classification accuracy (ranging from 77.5% to 97.5%) to separate different neurodegenerative disorders.

3.5. LIMITATIONS

The main limitation of this study is the small sample size, particularly of our SD and PNFA sub-groups. Thus, the results of this study cannot be easily transferred to the general populations of these patients. These disorders are relatively rare and, thus, high numbers of corresponding subjects cannot be easily recruited for the type of complex integrated unicenter PET/MRI study, which we performed here. However, we believe that the promising results of our study provide new insights despite the small sample size and, thus, would justify testing the approach discussed here in further (potentially multicenter) studies

on larger patient samples. Another limitation of this project is difference in age across groups, which was expected, as FTLD is typically an early onset disease compared to AD.

4. CONCLUSION:

Project-I: We provide evidence that: (i) intrinsic functional connectivity disruption between the hippocampus and the precuneus is consistently present in both Alzheimer's disease and mild cognitive impairment, (ii) local hypometabolism was obvious in the precuneus but glucose metabolism was relatively preserved in the hippocampus in Alzheimer's disease and mild cognitive impairment (iii) local atrophy has been seen in both the hippocampus and precuneus in Alzheimer's disease. Moreover, our findings demonstrated that, (iv) local metabolism of both regions rather than atrophy is associated with the functional connectivity, (v) There is an inverse correlation between the functional connectivity and hippocampus metabolism in Alzheimer's disease. Data are consistent with the hippocampus disconnection hypothesis of Alzheimer's disease, which suggests that with more functional disconnection from the precuneus, hippocampus metabolism is increased. This may reflect a loss of extra-hippocamal inhibitions or another pathological mechanism. Future longitudinal studies may aim to identify the temporal relationship between the different involved pathologies.

Project-II: Our findings suggest that the individual neuroimaging modalities based on the network degeneration hypothesis, including functional connectivity, glucose metabolism, grey matter volume and in particular the combination of these three modalities provide valid biomarkers to separate individual patients with distinct neurodegenerative diseases. The integrated neuroimaging method was superior for improving the clinical diagnosis of different dementia syndromes in comparison to a single modality. These results support further evidence for the network degeneration hypothesis of neurodegeneration.

5. REFERENCES

1. Reiman, E.M., et al., *Alzheimer's disease: implications of the updated diagnostic and research criteria.* J Clin Psychiatry, 2011. **72**(9): p. 1190-6.
2. Thies, W., L. Bleiler, and A. Alzheimer's, *2013 Alzheimer's disease facts and figures.* Alzheimers Dement, 2013. **9**(2): p. 208-45.
3. *American Psychiatric Association (2000). Diagnostic and statistical manual of mental disorders: DSM-IV-TR (4th Edition Text Revision ed.). Washington, DC: American Psychiatric Association.*
4. Jack, C.R., Jr., *Alzheimer disease: new concepts on its neurobiology and the clinical role imaging will play.* Radiology, 2012. **263**(2): p. 344-61.
5. Prince, M., et al., *The global prevalence of dementia: a systematic review and metaanalysis.* Alzheimers Dement, 2013. **9**(1): p. 63-75 e2.
6. Weber, M.M., *Aloys Alzheimer, a coworker of Emil Kraepelin.* J Psychiatr Res, 1997. **31**(6): p. 635-43.
7. McKhann, G.M., et al., *The diagnosis of dementia due to Alzheimer's disease: recommendations from the National Institute on Aging-Alzheimer's Association workgroups on diagnostic guidelines for Alzheimer's disease.* Alzheimers Dement, 2011. **7**(3): p. 263-9.
8. Brookmeyer, R., et al., *National estimates of the prevalence of Alzheimer's disease in the United States.* Alzheimers Dement, 2011. **7**(1): p. 61-73.
9. Fisher, G.G., et al., *Caring for individuals with dementia and cognitive impairment, not dementia: findings from the aging, demographics, and memory study.* J Am Geriatr Soc, 2011. **59**(3): p. 488-94.
10. Barnes, L.L., et al., *Gender, cognitive decline, and risk of AD in older persons.* Neurology, 2003. **60**(11): p. 1777-81.
11. Koepsell, T.D., et al., *Education, cognitive function, and severity of neuropathology in Alzheimer disease.* Neurology, 2008. **70**(19 Pt 2): p. 1732-9.
12. Roe, C.M., et al., *Education and Alzheimer disease without dementia: support for the cognitive reserve hypothesis.* Neurology, 2007. **68**(3): p. 223-8.
13. Dilworth-Anderson, P., et al., *Diagnosis and assessment of Alzheimer's disease in diverse populations.* Alzheimers Dement, 2008. **4**(4): p. 305-9.
14. Plassman, B.L., et al., *Prevalence of dementia in the United States: the aging, demographics, and memory study.* Neuroepidemiology, 2007. **29**(1-2): p. 125-32.
15. Honea, R.A., et al., *Maternal family history is associated with Alzheimer's disease biomarkers.* J Alzheimers Dis, 2012. **31**(3): p. 659-68.
16. Bertram, L. and R.E. Tanzi, *The genetics of Alzheimer's disease.* Prog Mol Biol Transl Sci, 2012. **107**: p. 79-100.
17. Ganguli, M., et al., *Outcomes of mild cognitive impairment by definition: a population study.* Arch Neurol, 2011. **68**(6): p. 761-7.
18. Luchsinger, J.A. and R. Mayeux, *Cardiovascular risk factors and Alzheimer's disease.* Curr Atheroscler Rep, 2004. **6**(4): p. 261-6.
19. Van Den Heuvel, C., E. Thornton, and R. Vink, *Traumatic brain injury and Alzheimer's disease: a review.* Prog Brain Res, 2007. **161**: p. 303-16.
20. Zanetti, O., S.B. Solerte, and F. Cantoni, *Life expectancy in Alzheimer's disease (AD).* Arch Gerontol Geriatr, 2009. **49 Suppl 1**: p. 237-43.

21. Nalivaeva, N.N., et al., *The Alzheimer's amyloid-degrading peptidase, neprilysin: can we control it?* Int J Alzheimers Dis, 2012. **2012**: p. 383796.
22. Shankar, G.M., et al., *Amyloid-beta protein dimers isolated directly from Alzheimer's brains impair synaptic plasticity and memory.* Nat Med, 2008. **14**(8): p. 837-42.
23. Hardy, J. and D. Allsop, *Amyloid deposition as the central event in the aetiology of Alzheimer's disease.* Trends Pharmacol Sci, 1991. **12**(10): p. 383-8.
24. Hardy, J. and D.J. Selkoe, *The amyloid hypothesis of Alzheimer's disease: progress and problems on the road to therapeutics.* Science, 2002. **297**(5580): p. 353-6.
25. Iqbal, K., et al., *Alzheimer's disease neurofibrillary degeneration: pivotal and multifactorial.* Biochem Soc Trans, 2010. **38**(4): p. 962-6.
26. Braak, H. and E. Braak, *Neuropathological stageing of Alzheimer-related changes.* Acta Neuropathol, 1991. **82**(4): p. 239-59.
27. Musiek, E.S. and D.M. Holtzman, *Origins of Alzheimer's disease: reconciling cerebrospinal fluid biomarker and neuropathology data regarding the temporal sequence of amyloid-beta and tau involvement.* Curr Opin Neurol, 2012. **25**(6): p. 715-20.
28. Price, J.L. and J.C. Morris, *Tangles and plaques in nondemented aging and "preclinical" Alzheimer's disease.* Ann Neurol, 1999. **45**(3): p. 358-68.
29. Tiraboschi, P., et al., *The importance of neuritic plaques and tangles to the development and evolution of AD.* Neurology, 2004. **62**(11): p. 1984-9.
30. Shepherd, C., H. McCann, and G.M. Halliday, *Variations in the neuropathology of familial Alzheimer's disease.* Acta Neuropathol, 2009. **118**(1): p. 37-52.
31. Mahley, R.W., K.H. Weisgraber, and Y. Huang, *Apolipoprotein E4: a causative factor and therapeutic target in neuropathology, including Alzheimer's disease.* Proc Natl Acad Sci U S A, 2006. **103**(15): p. 5644-51.
32. Rabinovici, G.D. and B.L. Miller, *Frontotemporal lobar degeneration: epidemiology, pathophysiology, diagnosis and management.* CNS Drugs, 2010. **24**(5): p. 375-98.
33. Weder, N.D., et al., *Frontotemporal dementias: a review.* Ann Gen Psychiatry, 2007. **6**: p. 15.
34. Barker, W.W., et al., *Relative frequencies of Alzheimer disease, Lewy body, vascular and frontotemporal dementia, and hippocampal sclerosis in the State of Florida Brain Bank.* Alzheimer Dis Assoc Disord, 2002. **16**(4): p. 203-12.
35. Roberson, E.D., et al., *Frontotemporal dementia progresses to death faster than Alzheimer disease.* Neurology, 2005. **65**(5): p. 719-25.
36. Snowden, J., D. Neary, and D. Mann, *Frontotemporal lobar degeneration: clinical and pathological relationships.* Acta Neuropathol, 2007. **114**(1): p. 31-8.
37. Litvan, I., *Therapy and management of frontal lobe dementia patients.* Neurology, 2001. **56**(11 Suppl 4): p. S41-5.
38. Rosso, S.M., et al., *Medical and environmental risk factors for sporadic frontotemporal dementia: a retrospective case-control study.* J Neurol Neurosurg Psychiatry, 2003. **74**(11): p. 1574-6.
39. Neary, D., et al., *Frontotemporal lobar degeneration: a consensus on clinical diagnostic criteria.* Neurology, 1998. **51**(6): p. 1546-54.
40. Neary, D., J. Snowden, and D. Mann, *Frontotemporal dementia.* Lancet Neurol, 2005. **4**(11): p. 771-80.
41. Piguet, O., et al., *Similar early clinical presentations in familial and non-familial frontotemporal dementia.* J Neurol Neurosurg Psychiatry, 2004. **75**(12): p. 1743-5.

42. Goedert, M., B. Ghetti, and M.G. Spillantini, *Frontotemporal dementia: implications for understanding Alzheimer disease.* Cold Spring Harb Perspect Med, 2012. **2**(2): p. a006254.
43. Galimberti, D. and E. Scarpini, *Genetics of frontotemporal lobar degeneration.* Front Neurol, 2012. **3**: p. 52.
44. Snyder, A.Z. and M.E. Raichle, *A brief history of the resting state: the Washington University perspective.* Neuroimage, 2012. **62**(2): p. 902-10.
45. Buxton, R.B., et al., *Modeling the hemodynamic response to brain activation.* Neuroimage, 2004. **23 Suppl 1**: p. S220-33.
46. Ogawa, S., et al., *Intrinsic signal changes accompanying sensory stimulation: functional brain mapping with magnetic resonance imaging.* Proc Natl Acad Sci U S A, 1992. **89**(13): p. 5951-5.
47. Wan, X., et al., *The neural basis of the hemodynamic response nonlinearity in human primary visual cortex: Implications for neurovascular coupling mechanism.* Neuroimage, 2006. **32**(2): p. 616-25.
48. Golanov, E.V. and D.J. Reis, *Nitric oxide and prostanoids participate in cerebral vasodilation elicited by electrical stimulation of the rostral ventrolateral medulla.* J Cereb Blood Flow Metab, 1994. **14**(3): p. 492-502.
49. Purdon, P.L. and R.M. Weisskoff, *Effect of temporal autocorrelation due to physiological noise and stimulus paradigm on voxel-level false-positive rates in fMRI.* Hum Brain Mapp, 1998. **6**(4): p. 239-49.
50. Biswal, B., et al., *Functional connectivity in the motor cortex of resting human brain using echo-planar MRI.* Magn Reson Med, 1995. **34**(4): p. 537-41.
51. Biswal, B.B., *Resting state fMRI: a personal history.* Neuroimage, 2012. **62**(2): p. 938-44.
52. Keller, C.J., et al., *Intrinsic functional architecture predicts electrically evoked responses in the human brain.* Proc Natl Acad Sci U S A, 2011. **108**(25): p. 10308-13.
53. Gardner, S.F., et al., *Principles and clinical applications of positron emission tomography.* Am J Hosp Pharm, 1992. **49**(6): p. 1499-506.
54. Magistretti, P.J., *Cellular bases of functional brain imaging: insights from neuron-glia metabolic coupling.* Brain Res, 2000. **886**(1-2): p. 108-112.
55. Drzezga, A., *Diagnosis of Alzheimer's disease with [18F]PET in mild and asymptomatic stages.* Behav Neurol, 2009. **21**(1): p. 101-15.
56. Lucignani, G. and F. Nobili, *FDG-PET for early assessment of Alzheimer's disease: isn't the evidence base large enough?* Eur J Nucl Med Mol Imaging, 2010. **37**(8): p. 1604-9.
57. Delso, G., et al., *Performance measurements of the Siemens mMR integrated whole-body PET/MR scanner.* J Nucl Med, 2011. **52**(12): p. 1914-22.
58. Zaidi, H., O. Mawlawi, and C.G. Orton, *Point/counterpoint. Simultaneous PET/MR will replace PET/CT as the molecular multimodality imaging platform of choice.* Med Phys, 2007. **34**(5): p. 1525-8.
59. Poole, M., et al., *Split gradient coils for simultaneous PET-MRI.* Magn Reson Med, 2009. **62**(5): p. 1106-11.
60. Gilbert, K.M., et al., *Evaluation of a positron emission tomography (PET)-compatible field-cycled MRI (FCMRI) scanner.* Magn Reson Med, 2009. **62**(4): p. 1017-25.
61. Schlemmer, H.P., et al., *Simultaneous MR/PET imaging of the human brain: feasibility study.* Radiology, 2008. **248**(3): p. 1028-35.

62. Drzezga, A., et al., *First clinical experience with integrated whole-body PET/MR: comparison to PET/CT in patients with oncologic diagnoses.* J Nucl Med, 2012. **53**(6): p. 845-55.
63. Eiber, M., et al., *Value of a Dixon-based MR/PET attenuation correction sequence for the localization and evaluation of PET-positive lesions.* Eur J Nucl Med Mol Imaging, 2011. **38**(9): p. 1691-701.
64. Catana, C., et al., *MRI-assisted PET motion correction for neurologic studies in an integrated MR-PET scanner.* J Nucl Med, 2011. **52**(1): p. 154-61.
65. Hitz, S., et al., *Systematic Comparison of the Performance of Integrated Whole-Body PET/MR Imaging to Conventional PET/CT for 18F-FDG Brain Imaging in Patients Examined for Suspected Dementia.* J Nucl Med, 2014.
66. Riedl, V., et al., *Local Activity Determines Functional Connectivity in the Resting Human Brain: A Simultaneous FDG-PET/fMRI Study.* J Neurosci, 2014. **34**(18): p. 6260-6.
67. Hofmann, M., et al., *Towards quantitative PET/MRI: a review of MR-based attenuation correction techniques.* Eur J Nucl Med Mol Imaging, 2009. **36 Suppl 1**: p. S93-104.
68. Martinez-Moller, A., et al., *Tissue classification as a potential approach for attenuation correction in whole-body PET/MRI: evaluation with PET/CT data.* J Nucl Med, 2009. **50**(4): p. 520-6.
69. Scahill, R.I., et al., *Mapping the evolution of regional atrophy in Alzheimer's disease: unbiased analysis of fluid-registered serial MRI.* Proc Natl Acad Sci U S A, 2002. **99**(7): p. 4703-7.
70. Killiany, R.J., et al., *MRI measures of entorhinal cortex vs hippocampus in preclinical AD.* Neurology, 2002. **58**(8): p. 1188-96.
71. Whitwell, J.L., et al., *MRI correlates of neurofibrillary tangle pathology at autopsy: a voxel-based morphometry study.* Neurology, 2008. **71**(10): p. 743-9.
72. Teipel, S.J., et al., *Relevance of magnetic resonance imaging for early detection and diagnosis of Alzheimer disease.* Med Clin North Am, 2013. **97**(3): p. 399-424.
73. Dubois, B., G. Picard, and M. Sarazin, *Early detection of Alzheimer's disease: new diagnostic criteria.* Dialogues Clin Neurosci, 2009. **11**(2): p. 135-9.
74. Johnson, K.A., et al., *Brain imaging in Alzheimer disease.* Cold Spring Harb Perspect Med, 2012. **2**(4): p. a006213.
75. Frisoni, G.B., et al., *Imaging markers for Alzheimer disease: which vs how.* Neurology, 2013. **81**(5): p. 487-500.
76. Sperling, R.A., et al., *Functional alterations in memory networks in early Alzheimer's disease.* Neuromolecular Med, 2010. **12**(1): p. 27-43.
77. Sperling, R.A., et al., *fMRI studies of associative encoding in young and elderly controls and mild Alzheimer's disease.* J Neurol Neurosurg Psychiatry, 2003. **74**(1): p. 44-50.
78. Dickerson, B.C., et al., *Medial temporal lobe function and structure in mild cognitive impairment.* Ann Neurol, 2004. **56**(1): p. 27-35.
79. Machulda, M.M., et al., *Comparison of memory fMRI response among normal, MCI, and Alzheimer's patients.* Neurology, 2003. **61**(4): p. 500-6.
80. O'Brien, J.L., et al., *Longitudinal fMRI in elderly reveals loss of hippocampal activation with clinical decline.* Neurology, 2010. **74**(24): p. 1969-76.
81. Rosenberg, P.B. and C. Lyketsos, *Mild cognitive impairment: searching for the prodrome of Alzheimer's disease.* World Psychiatry, 2008. **7**(2): p. 72-8.

82. Miller, S.L., et al., *Hippocampal activation in adults with mild cognitive impairment predicts subsequent cognitive decline.* J Neurol Neurosurg Psychiatry, 2008. **79**(6): p. 630-5.
83. Bakker, A., et al., *Reduction of hippocampal hyperactivity improves cognition in amnestic mild cognitive impairment.* Neuron, 2012. **74**(3): p. 467-74.
84. Sorg, C., et al., *Selective changes of resting-state networks in individuals at risk for Alzheimer's disease.* Proc Natl Acad Sci U S A, 2007. **104**(47): p. 18760-5.
85. Kim, J., Y.H. Kim, and J.H. Lee, *Hippocampus-precuneus functional connectivity as an early sign of Alzheimer's disease: a preliminary study using structural and functional magnetic resonance imaging data.* Brain Res, 2013. **1495**: p. 18-29.
86. Greicius, M.D., et al., *Default-mode network activity distinguishes Alzheimer's disease from healthy aging: evidence from functional MRI.* Proc Natl Acad Sci U S A, 2004. **101**(13): p. 4637-42.
87. Buckner, R.L., J.R. Andrews-Hanna, and D.L. Schacter, *The brain's default network: anatomy, function, and relevance to disease.* Ann N Y Acad Sci, 2008. **1124**: p. 1-38.
88. Zhou, Y., et al., *Abnormal connectivity in the posterior cingulate and hippocampus in early Alzheimer's disease and mild cognitive impairment.* Alzheimers Dement, 2008. **4**(4): p. 265-70.
89. Sperling, R.A., et al., *Amyloid deposition is associated with impaired default network function in older persons without dementia.* Neuron, 2009. **63**(2): p. 178-88.
90. Sheline, Y.I., et al., *Amyloid plaques disrupt resting state default mode network connectivity in cognitively normal elderly.* Biol Psychiatry, 2010. **67**(6): p. 584-7.
91. Myers, N., et al., *Within-patient correspondence of amyloid-beta and intrinsic network connectivity in Alzheimer's disease.* Brain, 2014.
92. Drzezga, A., et al., *Neuronal dysfunction and disconnection of cortical hubs in non-demented subjects with elevated amyloid burden.* Brain, 2011. **134**(Pt 6): p. 1635-46.
93. Rombouts, S.A., et al., *Alterations in brain activation during cholinergic enhancement with rivastigmine in Alzheimer's disease.* J Neurol Neurosurg Psychiatry, 2002. **73**(6): p. 665-71.
94. Shanks, M.F., et al., *Regional brain activity after prolonged cholinergic enhancement in early Alzheimer's disease.* Magn Reson Imaging, 2007. **25**(6): p. 848-59.
95. Saykin, A.J., et al., *Cholinergic enhancement of frontal lobe activity in mild cognitive impairment.* Brain, 2004. **127**(Pt 7): p. 1574-83.
96. Bokde, A.L., et al., *Decreased activation along the dorsal visual pathway after a 3-month treatment with galantamine in mild Alzheimer disease: a functional magnetic resonance imaging study.* J Clin Psychopharmacol, 2009. **29**(2): p. 147-56.
97. Drzezga, A., et al., *Prediction of individual clinical outcome in MCI by means of genetic assessment and (18)F-FDG PET.* J Nucl Med, 2005. **46**(10): p. 1625-32.
98. Del Sole, A., et al., *Individual cerebral metabolic deficits in Alzheimer's disease and amnestic mild cognitive impairment: an FDG PET study.* Eur J Nucl Med Mol Imaging, 2008. **35**(7): p. 1357-66.
99. Mosconi, L., et al., *Hypometabolism exceeds atrophy in presymptomatic early-onset familial Alzheimer's disease.* J Nucl Med, 2006. **47**(11): p. 1778-86.
100. Mosconi, L., et al., *FDG-PET changes in brain glucose metabolism from normal cognition to pathologically verified Alzheimer's disease.* Eur J Nucl Med Mol Imaging, 2009. **36**(5): p. 811-22.

101. de Leon, M.J., et al., *Prediction of cognitive decline in normal elderly subjects with 2-[(18)F]fluoro-2-deoxy-D-glucose/poitron-emission tomography (FDG/PET).* Proc Natl Acad Sci U S A, 2001. **98**(19): p. 10966-71.
102. Samuraki, M., et al., *Partial volume effect-corrected FDG PET and grey matter volume loss in patients with mild Alzheimer's disease.* Eur J Nucl Med Mol Imaging, 2007. **34**(10): p. 1658-69.
103. Ishii, K., et al., *Relatively preserved hippocampal glucose metabolism in mild Alzheimer's disease.* Dement Geriatr Cogn Disord, 1998. **9**(6): p. 317-22.
104. Mevel, K., et al., *Detecting hippocampal hypometabolism in Mild Cognitive Impairment using automatic voxel-based approaches.* Neuroimage, 2007. **37**(1): p. 18-25.
105. Villain, N., et al., *Sequential relationships between grey matter and white matter atrophy and brain metabolic abnormalities in early Alzheimer's disease.* Brain, 2010. **133**(11): p. 3301-14.
106. Chetelat, G., et al., *Direct voxel-based comparison between grey matter hypometabolism and atrophy in Alzheimer's disease.* Brain, 2008. **131**(Pt 1): p. 60-71.
107. Villain, N., et al., *Relationships between hippocampal atrophy, white matter disruption, and gray matter hypometabolism in Alzheimer's disease.* J Neurosci, 2008. **28**(24): p. 6174-81.
108. Jagust, W., *Positron emission tomography and magnetic resonance imaging in the diagnosis and prediction of dementia.* Alzheimers Dement, 2006. **2**(1): p. 36-42.
109. Forster, S., et al., *Effects of a 6-month cognitive intervention on brain metabolism in patients with amnestic MCI and mild Alzheimer's disease.* J Alzheimers Dis, 2011. **26 Suppl 3**: p. 337-48.
110. de Wilde, M.C., et al., *Utility of imaging for nutritional intervention studies in Alzheimer's disease.* Eur J Pharmacol, 2011. **668 Suppl 1**: p. S59-69.
111. Rabinovici, G.D., et al., *Amyloid vs FDG-PET in the differential diagnosis of AD and FTLD.* Neurology, 2011. **77**(23): p. 2034-42.
112. Engler, H., et al., *Two-year follow-up of amyloid deposition in patients with Alzheimer's disease.* Brain, 2006. **129**(Pt 11): p. 2856-66.
113. Celone, K.A., et al., *Alterations in memory networks in mild cognitive impairment and Alzheimer's disease: an independent component analysis.* J Neurosci, 2006. **26**(40): p. 10222-31.
114. Walhovd, K.B., et al., *Combining MR imaging, positron-emission tomography, and CSF biomarkers in the diagnosis and prognosis of Alzheimer disease.* AJNR Am J Neuroradiol, 2010. **31**(2): p. 347-54.
115. Petrie, E.C., et al., *Preclinical evidence of Alzheimer changes: convergent cerebrospinal fluid biomarker and fluorodeoxyglucose positron emission tomography findings.* Arch Neurol, 2009. **66**(5): p. 632-7.
116. Schroeter, M.L., et al., *Neural networks in frontotemporal dementia--a meta-analysis.* Neurobiol Aging, 2008. **29**(3): p. 418-26.
117. Seeley, W.W., et al., *Frontal paralimbic network atrophy in very mild behavioral variant frontotemporal dementia.* Arch Neurol, 2008. **65**(2): p. 249-55.
118. Zhou, J., et al., *Divergent network connectivity changes in behavioural variant frontotemporal dementia and Alzheimer's disease.* Brain, 2010. **133**(Pt 5): p. 1352-67.

119. Davies, R.R., et al., *Progression in frontotemporal dementia: identifying a benign behavioral variant by magnetic resonance imaging.* Arch Neurol, 2006. **63**(11): p. 1627-31.
120. Kipps, C.M., et al., *Combined magnetic resonance imaging and positron emission tomography brain imaging in behavioural variant frontotemporal degeneration: refining the clinical phenotype.* Brain, 2009. **132**(Pt 9): p. 2566-78.
121. Kipps, C.M., J.R. Hodges, and M. Hornberger, *Nonprogressive behavioural frontotemporal dementia: recent developments and clinical implications of the 'bvFTD phenocopy syndrome'.* Curr Opin Neurol, 2010. **23**(6): p. 628-32.
122. Seeley, W.W., et al., *Neurodegenerative diseases target large-scale human brain networks.* Neuron, 2009. **62**(1): p. 42-52.
123. Davies, R.R., et al., *The human perirhinal cortex and semantic memory.* Eur J Neurosci, 2004. **20**(9): p. 2441-6.
124. Rohrer, J.D., et al., *Patterns of cortical thinning in the language variants of frontotemporal lobar degeneration.* Neurology, 2009. **72**(18): p. 1562-9.
125. Gorno-Tempini, M.L., et al., *Cognition and anatomy in three variants of primary progressive aphasia.* Ann Neurol, 2004. **55**(3): p. 335-46.
126. Nestor, P.J., et al., *Progressive non-fluent aphasia is associated with hypometabolism centred on the left anterior insula.* Brain, 2003. **126**(Pt 11): p. 2406-18.
127. Rogalski, E., et al., *Progression of language decline and cortical atrophy in subtypes of primary progressive aphasia.* Neurology, 2011. **76**(21): p. 1804-10.
128. Gunawardena, D., et al., *Why are patients with progressive nonfluent aphasia nonfluent?* Neurology, 2010. **75**(7): p. 588-94.
129. Agosta, F., et al., *Brain network connectivity assessed using graph theory in frontotemporal dementia.* Neurology, 2013. **81**(2): p. 134-43.
130. Viard, A., et al., *Autobiographical memory in semantic dementia: new insights from two patients using fMRI.* Neuropsychologia, 2013. **51**(13): p. 2620-32.
131. Cooke, A., et al., *Neural basis for sentence comprehension deficits in frontotemporal dementia.* Brain Lang, 2003. **85**(2): p. 211-21.
132. Grimmer, T., et al., *Region-specific decline of cerebral glucose metabolism in patients with frontotemporal dementia: a prospective 18F-FDG-PET study.* Dement Geriatr Cogn Disord, 2004. **18**(1): p. 32-6.
133. Diehl, J., et al., *Cerebral metabolic patterns at early stages of frontotemporal dementia and semantic dementia. A PET study.* Neurobiol Aging, 2004. **25**(8): p. 1051-6.
134. Diehl-Schmid, J., et al., *Decline of cerebral glucose metabolism in frontotemporal dementia: a longitudinal 18F-FDG-PET-study.* Neurobiol Aging, 2007. **28**(1): p. 42-50.
135. Drzezga, A., et al., *Imaging of amyloid plaques and cerebral glucose metabolism in semantic dementia and Alzheimer's disease.* Neuroimage, 2008. **39**(2): p. 619-33.
136. Perneczky, R., et al., *Non-fluent progressive aphasia: cerebral metabolic patterns and brain reserve.* Brain Res, 2007. **1133**(1): p. 178-85.
137. Wilson, S.M., et al., *Automated MRI-based classification of primary progressive aphasia variants.* Neuroimage, 2009. **47**(4): p. 1558-67.
138. Munoz-Ruiz, M.A., et al., *Structural MRI in frontotemporal dementia: comparisons between hippocampal volumetry, tensor-based morphometry and voxel-based morphometry.* PLoS One, 2012. **7**(12): p. e52531.

139. Pereira, J.M., et al., *Atrophy patterns in histologic vs clinical groupings of frontotemporal lobar degeneration.* Neurology, 2009. **72**(19): p. 1653-60.
140. Zhang, Y., et al., *MRI signatures of brain macrostructural atrophy and microstructural degradation in frontotemporal lobar degeneration subtypes.* J Alzheimers Dis, 2013. **33**(2): p. 431-44.
141. Foster, N.L., et al., *FDG-PET improves accuracy in distinguishing frontotemporal dementia and Alzheimer's disease.* Brain, 2007. **130**(Pt 10): p. 2616-35.
142. Schroeter, M.L. and J. Neumann, *Combined Imaging Markers Dissociate Alzheimer's Disease and Frontotemporal Lobar Degeneration - An ALE Meta-Analysis.* Front Aging Neurosci, 2011. **3**: p. 10.
143. Dukart, J., et al., *Meta-analysis based SVM classification enables accurate detection of Alzheimer's disease across different clinical centers using FDG-PET and MRI.* Psychiatry Res, 2013. **212**(3): p. 230-6.
144. Dukart, J., et al., *Combined evaluation of FDG-PET and MRI improves detection and differentiation of dementia.* PLoS One, 2011. **6**(3): p. e18111.
145. Pasquini L, S.M., Tahmasian M, Meng C, Myers NE, Ortner M, Mühlau M, Kurz A, Förstl H, Zimmer C, Grimmer T, Wohlschläger AM, Riedl V, Sorg C, *Link between hippocampus' raised local and eased global intrinsic connectivity in AD.* Alzheimer and dementia, 2014.
146. Das, S.R., et al., *Increased functional connectivity within medial temporal lobe in mild cognitive impairment.* Hippocampus, 2013. **23**(1): p. 1-6.
147. Buckner, R.L., et al., *Molecular, structural, and functional characterization of Alzheimer's disease: evidence for a relationship between default activity, amyloid, and memory.* J Neurosci, 2005. **25**(34): p. 7709-17.
148. Rombouts, S.A., et al., *Altered resting state networks in mild cognitive impairment and mild Alzheimer's disease: an fMRI study.* Hum Brain Mapp, 2005. **26**(4): p. 231-9.
149. Zhang, H.Y., et al., *Resting brain connectivity: changes during the progress of Alzheimer disease.* Radiology, 2010. **256**(2): p. 598-606.
150. He, Y., et al., *Regional coherence changes in the early stages of Alzheimer's disease: a combined structural and resting-state functional MRI study.* Neuroimage, 2007. **35**(2): p. 488-500.
151. Wang, L., et al., *Changes in hippocampal connectivity in the early stages of Alzheimer's disease: evidence from resting state fMRI.* Neuroimage, 2006. **31**(2): p. 496-504.
152. Morbelli, S., et al., *Mapping brain morphological and functional conversion patterns in amnestic MCI: a voxel-based MRI and FDG-PET study.* Eur J Nucl Med Mol Imaging, 2010. **37**(1): p. 36-45.
153. Riha, P.D., et al., *Animal model of posterior cingulate cortex hypometabolism implicated in amnestic MCI and AD.* Neurobiol Learn Mem, 2008. **90**(1): p. 112-24.
154. Li, Y., et al., *Regional analysis of FDG and PIB-PET images in normal aging, mild cognitive impairment, and Alzheimer's disease.* Eur J Nucl Med Mol Imaging, 2008. **35**(12): p. 2169-81.
155. van de Pol, L.A., et al., *Hippocampal atrophy in Alzheimer disease: age matters.* Neurology, 2006. **66**(2): p. 236-8.
156. Spulber, G., et al., *An MRI-based index to measure the severity of Alzheimer's disease-like structural pattern in subjects with mild cognitive impairment.* J Intern Med, 2013. **273**(4): p. 396-409.

157. Zimny, A., et al., *Quantitative MR evaluation of atrophy, as well as perfusion and diffusion alterations within hippocampi in patients with Alzheimer's disease and mild cognitive impairment.* Med Sci Monit, 2013. **19**: p. 86-94.
158. Chetelat, G., et al., *Relationship between atrophy and beta-amyloid deposition in Alzheimer disease.* Ann Neurol, 2010. **67**(3): p. 317-24.
159. Bourgeat, P., et al., *Beta-amyloid burden in the temporal neocortex is related to hippocampal atrophy in elderly subjects without dementia.* Neurology, 2010. **74**(2): p. 121-7.
160. Yakushev, I., et al., *Functional implications of hippocampal degeneration in early Alzheimer's disease: a combined DTI and PET study.* Eur J Nucl Med Mol Imaging, 2011. **38**(12): p. 2219-27.
161. Welsh, K.A., et al., *The Consortium to Establish a Registry for Alzheimer's Disease (CERAD). Part V. A normative study of the neuropsychological battery.* Neurology, 1994. **44**(4): p. 609-14.
162. Winblad, B., et al., *Mild cognitive impairment--beyond controversies, towards a consensus: report of the International Working Group on Mild Cognitive Impairment.* J Intern Med, 2004. **256**(3): p. 240-6.
163. Tahmasian, M., et al., *Aberrant intrinsic connectivity of hippocampus and amygdala overlap in the fronto-insular and dorsomedial-prefrontal cortex in major depressive disorder.* Front Hum Neurosci, 2013. **7**: p. 639.
164. Sorg, C., et al., *Increased intrinsic brain activity in the striatum reflects symptom dimensions in schizophrenia.* Schizophr Bull, 2013. **39**(2): p. 387-95.
165. Van Dijk, K.R., M.R. Sabuncu, and R.L. Buckner, *The influence of head motion on intrinsic functional connectivity MRI.* Neuroimage, 2012. **59**(1): p. 431-8.
166. Kahn, I., et al., *Distinct cortical anatomy linked to subregions of the medial temporal lobe revealed by intrinsic functional connectivity.* J Neurophysiol, 2008. **100**(1): p. 129-39.
167. Ashburner, J. and K.J. Friston, *Unified segmentation.* Neuroimage, 2005. **26**(3): p. 839-51.
168. Marrelec, G., et al., *Partial correlation for functional brain interactivity investigation in functional MRI.* Neuroimage, 2006. **32**(1): p. 228-37.
169. Pozueta, J., R. Lefort, and M.L. Shelanski, *Synaptic changes in Alzheimer's disease and its models.* Neuroscience, 2013. **251**: p. 51-65.
170. de Calignon, A., et al., *Propagation of tau pathology in a model of early Alzheimer's disease.* Neuron, 2012. **73**(4): p. 685-97.
171. Reyes, J.F., N.L. Rey, and E. Angot, *Transmission of tau pathology induced by synthetic preformed tau filaments.* J Neurosci, 2013. **33**(16): p. 6707-8.
172. Clavaguera, F., et al., *Transmission and spreading of tauopathy in transgenic mouse brain.* Nat Cell Biol, 2009. **11**(7): p. 909-13.
173. Stricker, N.H., et al., *CSF biomarker associations with change in hippocampal volume and precuneus thickness: implications for the Alzheimer's pathological cascade.* Brain Imaging Behav, 2012. **6**(4): p. 599-609.
174. Moller, C., et al., *Different patterns of gray matter atrophy in early- and late-onset Alzheimer's disease.* Neurobiol Aging, 2013. **34**(8): p. 2014-22.
175. Putcha, D., et al., *Hippocampal hyperactivation associated with cortical thinning in Alzheimer's disease signature regions in non-demented elderly adults.* J Neurosci, 2011. **31**(48): p. 17680-8.

176. Wilson, I.A., et al., *Neurocognitive aging: prior memories hinder new hippocampal encoding.* Trends Neurosci, 2006. **29**(12): p. 662-70.
177. Yassa, M.A., et al., *High-resolution structural and functional MRI of hippocampal CA3 and dentate gyrus in patients with amnestic Mild Cognitive Impairment.* Neuroimage, 2010. **51**(3): p. 1242-52.
178. Hyman, B.T., P.J. Eslinger, and A.R. Damasio, *Effect of naltrexone on senile dementia of the Alzheimer type.* J Neurol Neurosurg Psychiatry, 1985. **48**(11): p. 1169-71.
179. Bak, T.H. and S. Chandran, *What wires together dies together: verbs, actions and neurodegeneration in motor neuron disease.* Cortex, 2012. **48**(7): p. 936-44.
180. Frost, B. and M.I. Diamond, *Prion-like mechanisms in neurodegenerative diseases.* Nat Rev Neurosci, 2010. **11**(3): p. 155-9.
181. Eidelberg, D. and W. Martin, *Different beta-amyloid binding patterns in Alzheimer and Parkinson diseases: it's the network!* Neurology, 2013. **81**(6): p. 516-7.
182. Frisch, S., et al., *Dissociating memory networks in early Alzheimer's disease and frontotemporal lobar degeneration - a combined study of hypometabolism and atrophy.* PLoS One, 2013. **8**(2): p. e55251.
183. McKhann, G.M., et al., *Clinical and pathological diagnosis of frontotemporal dementia: report of the Work Group on Frontotemporal Dementia and Pick's Disease.* Arch Neurol, 2001. **58**(11): p. 1803-9.
184. Hindmarch, I., et al., *The Bayer Activities of Daily Living Scale (B-ADL).* Dement Geriatr Cogn Disord, 1998. **9 Suppl 2**: p. 20-6.
185. Kloppel, S., et al., *Automatic classification of MR scans in Alzheimer's disease.* Brain, 2008. **131**(Pt 3): p. 681-9.
186. Buckner, R.L., et al., *Cortical hubs revealed by intrinsic functional connectivity: mapping, assessment of stability, and relation to Alzheimer's disease.* J Neurosci, 2009. **29**(6): p. 1860-73.
187. Wang, J.H., et al., *Graph theoretical analysis of functional brain networks: test-retest evaluation on short- and long-term resting-state functional MRI data.* PLoS One, 2011. **6**(7): p. e21976.
188. Dawson, N., et al., *Sustained NMDA receptor hypofunction induces compromised neural systems integration and schizophrenia-like alterations in functional brain networks.* Cereb Cortex, 2014. **24**(2): p. 452-64.
189. Meng, C., et al., *Aberrant topology of striatum's connectivity is associated with the number of episodes in depression.* Brain, 2014. **137**(Pt 2): p. 598-609.
190. Zuo, X.N., et al., *Network centrality in the human functional connectome.* Cereb Cortex, 2012. **22**(8): p. 1862-75.
191. Song, X.W., et al., *REST: a toolkit for resting-state functional magnetic resonance imaging data processing.* PLoS One, 2011. **6**(9): p. e25031.
192. Shao, J., et al., *Prediction of Alzheimer's disease using individual structural connectivity networks.* Neurobiol Aging, 2012. **33**(12): p. 2756-65.
193. Boccardi, M., et al., *Frontotemporal dementia as a neural system disease.* Neurobiol Aging, 2005. **26**(1): p. 37-44.
194. Gomez-Ramirez, J. and J. Wu, *Network-based biomarkers in Alzheimer's disease: review and future directions.* Front Aging Neurosci, 2014. **6**: p. 12.
195. Clark, C.M., et al., *Biomarkers for early detection of Alzheimer pathology.* Neurosignals, 2008. **16**(1): p. 11-8.

196. Habeck, C., et al., *Multivariate and univariate neuroimaging biomarkers of Alzheimer's disease.* Neuroimage, 2008. **40**(4): p. 1503-15.
197. Habert, M.O., et al., *Brain perfusion SPECT correlates with CSF biomarkers in Alzheimer's disease.* Eur J Nucl Med Mol Imaging, 2010. **37**(3): p. 589-93.
198. Wee, C.Y., et al., *Resting-state multi-spectrum functional connectivity networks for identification of MCI patients.* PLoS One, 2012. **7**(5): p. e37828.
199. Chhatwal, J.P., et al., *Impaired default network functional connectivity in autosomal dominant Alzheimer disease.* Neurology, 2013. **81**(8): p. 736-44.
200. Filippi, M., et al., *Functional network connectivity in the behavioral variant of frontotemporal dementia.* Cortex, 2013. **49**(9): p. 2389-401.
201. Herholz, K., *Use of FDG PET as an imaging biomarker in clinical trials of Alzheimer's disease.* Biomark Med, 2012. **6**(4): p. 431-9.
202. Poljansky, S., et al., *A visual [18F]FDG-PET rating scale for the differential diagnosis of frontotemporal lobar degeneration.* Eur Arch Psychiatry Clin Neurosci, 2011. **261**(6): p. 433-46.

6. PUBLICATIONS

1. Publications derived from this thesis

- Tahmasian M, Pasquini L, Meng C, Förster S, Bratec S, Shi K, Yakushev I, Grimemr T, Diehl-Schmid J, Riedl V, Schwaiger M, Sorg C, Drzezga A. Inverse link between hippocampus reduced connectivity and its metabolism in Alzheimer's disease, 2014 [Under revision].

- Tahmasian M, Meng C, Grimemr T, Diehl-Schmid J, Förster S, Riedl V, Schwaiger M, Drzezga A, Sorg C. Separation of distinct neurodegenerative diseases based on network degeneration hypothesis: a PET/MRI study, 2014 [Under revision].

2. Congress presentations derived from this thesis

- Tahmasian M, Sorg C, Meng C, Grimemr T, Diehl-Schmid J, Pasquini L, Bratec S, Förster S, Yakushev I, Yousefi B, Riedl V, Schwaiger M, Drzezga A. Association between metabolic and structural changes of hippocampus and retrosplenial cortex with disruption of functional connectivity in Alzheimer's disease and mild cognitive impairment: a PET/MR study, Annual meeting of Society *for Neuroscience*, San Diego, USA, 9-13 November 2013.

- Tahmasian M, Meng C, Shao J, Grimemr T, Diehl-Schmid J, Riedl V, Förster S, Schwaiger M, Drzezga A, Sorg C. Separation of neurodegenerative diseases based on the network degeneration hypothesis: PET/MRI study, Annual meeting of the Organization for Human Brain Mapping, Hamburg, Germany, 8-12 June 2014.

3. Further publications on neuroimaging, which are not part of this thesis

- Pasquini L, Scherr M, Tamashian M, Akhrif A, Myers N, Ortner M, Mühlau M, Kurz A, Förstl H, Zimmer C, Grimmer T, Wohlschläger A.M, Riedl V, Sorg C. Raised ongoing

activity in hippocampal subfields links with cortical thinning in Alzheimer's disease, 2014 [Under revision].

- Pasquini L, Scherr M, Tamashian M, Meng C, Myers N, Ortner M, Mühlau M, Kurz A, Förstl H, Zimmer C, Grimmer T, Wohlschläger A.M, Riedl V, Sorg C. Selectively and progressively increased BOLD synchrony within the hippocampus in Alzheimer's disease, *Alzheimer and dementia*, 2014 Jul 17. pii: S1552-5260(14)02415-7. doi: 10.1016/j.jalz.2014.02.007.

- Klupp E, Förster S, Grimmer T, Tahmasian M, Sorg C, Yousefi B, Drzezga A. In Alzheimer's disease, hypometabolism in low-amyloid brain regions may be a functional consequence of pathologies in connected brain regions, *Brain connectivity*, 2014 Jun;4(5):371-83. doi: 10.1089/brain.2013.0212.

- Riedl V, Bienkowska K, Strobel C, Tahmasian M, Grimmer T, Förster S, Friston K.J, Sorg C, Drzezga A. Local activity determines functional connectivity in the resting human brain, *Journal of neuroscience*, *Journal of neuroscience*, 2014 Apr 30;34(18):6260-6. doi: 10.1523/JNEUROSCI.0492-14.2014.

- Manoliu A, Meng C, Brandl F, Doll A, Tahmasian M, Zimmer C, Förstl H, Bäuml J, Wohlschläger A, Riedl V, Sorg C. Insular dysfunction within salience network is associated with severity of symptoms and aberrant inter-network connectivity in major depressive disorder severity of symptoms in depression, *Frontier of human neuroscience*, 2014 014 Jan 21;7:930. doi: 10.3389/fnhum.2013.00930. eCollection 2013.

- Meng C, Brandl F, Tahmasian M, Shao J, Manoliu A, Scherr M, Schwerthöffer D, Bäuml J, Förstl H, Zimmer C, Wohlschläger A.M, Riedl V, Sorg C. Aberrant putamen intrinsic network topology links with the number of episodes in major depression, *Brain*, 2013 Oct 26. doi: 10.1093/brain/awt290.

- Tahmasian M, Knight D.C, Manoliu A, Schwerthöffer D, Meng C, Shao J, Peters H, Doll A, Khazaie H, Mueller M, Drzezga A, Bäuml J, Zimmer C, Förstl H, Wohlschläger AM, Riedl V, Sorg C. Aberrant intrinsic connectivity of hippocampus and amygdala overlap in the fronto-insular and dorsomedial-prefrontal cortex in major depressive disorder. *Frontier of human neuroscience*, 2013 01 October. doi:10.3389/fnhum.2013.00639.

6. ACKNOWLEDGEMENT

I would like to thank my supervisor Prof. Dr. med. Alexander Drzezga for his kind support and advice throughout my doctorate, for encouraging my research, and for allowing me to grow as a researcher.

I also thank my co-supervisor Prof. Dr. med. Claus Zimmer for his support, for having offered me the possibility to work in such an excellent environment, and for encouraging me to undertake this honorable PhD program.

I would like to express my sincere gratitude to Dr. med. Christian Sorg and Dr. med. Valentin Riedl, Ph.D. for the introduction of resting-state fMRI and for their friendly and professional support. Without their supervision and constant help, accomplishing this dissertation would not have been possible.

I am very thankful to Dr. med. Stefan Förster and Dr. Behrooz H. Yousefi PhD for their scientific support and also Dr. med. Katrin Offe and Ms. Desislava Zlatanova for their friendly and patient support regarding administrative and academic questions.

Thanks a lot to all participants who contributed to these studies. I, particularly, appreciate all patients who volunteered to participate in this study, despite their illness.

Last but not least, I am deeply grateful to my lovely parents, as well as Farnoosh Emamian for their kindness and strong support and their patience throughout my studies.